

Potent inhibitors of human LAT1 (SLC7A5) transporter based on dithiazole and dithiazine compounds for development of anticancer drugs

Lara Napolitano^{a1}, Mariafrancesca Scalise^{a1}, Maria Koyioni^b, Panayotis Koutentis^b, Marco Catto^c, Ivano Eberini^d, Chiara Parravicini^d, Luca Palazzolo^e, Leonardo Pisani^c, Michele Galluccio^a, Lara Console^a, Angelo Carotti^c and Cesare Indiveri^{a*}.

^aDepartment DiBEST (Biologia, Ecologia, Scienze della Terra) Unit of Biochemistry and Molecular Biotechnology, University of Calabria, Via P. Bucci 4C, 87036 Arcavacata di Rende, Italy

^bDepartment of Chemistry, University of Cyprus, P.O. Box 20537, 1678 Nicosia, Cyprus

^cDipartimento Farmaco-Chimico, Università degli Studi “Aldo Moro,” via Orabona 4, 70125 Bari, Italy

^dDipartimento di Scienze Farmacologiche e Biomolecolari, Università degli Studi di Milano, Italy

^eDipartimento di Scienze Farmacologiche e Biomolecolari e Dipartimento di Scienze Biomediche e Cliniche “L. Sacco”, Università degli Studi di Milano, Italy

¹These authors contributed equally to this work

*Corresponding author. E-mail addresses: cesare.indiveri@unical.it (C. Indiveri)

ABSTRACT

1
2 The effect of dithiazole and dithiazine compounds on the human (h)LAT1 transporter has been
3
4 screened in proteoliposomes. Inhibition was tested on the antiport catalysed by hLAT1 as transport
5
6 of extraliposomal [³H]histidine in exchange with intraliposomal histidine. Out of 59 compounds
7
8 tested, 8 compounds, showing an inhibition higher than 90% at 100 μM concentration, were
9
10 subjected to dose-response analysis. Two of them exhibited IC₅₀ lower than 1 μM. Inhibition
11
12 kinetics, performed on the two best inhibitors, resulted in a mixed type inhibition with respect to the
13
14 substrate. Furthermore, inhibition of the transporter was still present after removal of compounds
15
16 from the reaction mixture, but was reversed on addition of dithioerythritol, a S-S reducing agent,
17
18 indicating the involvement of disulfide(s) between the compounds and the protein. Molecular
19
20 docking of the two best inhibitors on the hLAT1 homology structural model, highlighted interaction
21
22 with the substrate binding site and formation of a covalent bond with the residue C407. Indeed, the
23
24 inhibition was impaired in the hLAT1 mutant C407A confirming the involvement of that Cys
25
26 residue. Treatment of SiHa cells expressing hLAT1 at relatively high level, with the two most
27
28 potent inhibitors led to cell death which was not observed after treatment with a compound
29
30 exhibiting very poor inhibitory potency.
31
32
33
34
35
36
37
38
39
40

41 **Abbreviations:** LAT, L-type amino acid transporters 1; SLC, Solute carrier; CD98, cluster of
42
43 differentiation 98; ASCT2, AlaSerCys Transporter 2; mTOR, mammalian target of rapamycin;
44
45 BBB, blood brain barrier; AdiC, L-arginine/agmatine antiporter, C₁₂E₈, octaethylene glycol
46
47 monododecyl ether; BCH, 2-amino-2-norbornanecarboxylic acid; DTE, dithioerythritol; TX-100,
48
49 Triton X-100
50
51
52
53
54
55

56 **Keywords:** LAT1 inhibitors; 1,2,3-dithiazoles; 1,2,4-dithiazines; mechanism of inhibition;
57
58 pharmacological target; cancer.
59
60
61
62
63
64
65

1. Introduction

LAT1 (SLC7A5) is a branched chain and aromatic amino acid transporter belonging to the Heterodimeric Amino acid Transporter group (HATs). Structurally, it is characterized by the association of the light chain LAT1 with the glycoprotein CD98 (SLC3A2). The interaction between the two proteins occurs through a conserved disulfide bond between C164 and C109 of the human isoforms of LAT1 and CD98, respectively [1]. The structure of CD98 has been solved by X-ray crystallography [2] while that of LAT1 has been only predicted by homology modeling [3, 4]. Recently, LAT1 was demonstrated to be the sole transport competent subunit, able to recognize His as one of the major substrates. Transport is not dependent on sodium gradient or on pH [3, 5]. LAT1 gives rise to an antiport reaction that follows a random simultaneous mechanism in which amino acids bind with no preferential order to the transporter. The substrate binding site is characterized by the key residues F252, S342, C335 and C407. In particular, F252 is the gate element that allows substrate entry, while S342 and C335 are involved in substrate binding prior to translocation [3]. LAT1 is localized in several body districts among which, the Blood Brain Barrier where it regulates the exchange of eight out of nine essential amino acids. Alteration of this function, was recently shown to cause Autism Spectrum Disorders [5]. Concerning its sub-cellular localization, LAT1 is mainly expressed at the plasma membrane but its presence in lysosomal membrane has also been reported [6]. In this organelle, the transporter may play a role in cell signaling, as demonstrated for SLC38A9 which transduces Gln and Arg sufficiency to mTORC1 [7, 8]. Nevertheless, trafficking of LAT1 to these alternative cell localizations remains to be better defined.

The biomedical and pharmacological interest on LAT1 resides in its over-expression in many tumors [9]. In fact, due to its specificity also for Gln, it is involved in “Glutamine addiction”, a typical feature of tumor cells that use Gln for energy purpose at a much higher rate than normal cells. In this respect, LAT1 realizes a Gln/Leu cycle in concert with another transporter, namely ASCT2 that is a Na⁺-dependent antiporter for Gln and other neutral amino acids. Therefore, both

1 transporters are involved in cancer growth and progression [10]. LAT1 is, indeed, considered as a
2 marker of malignancy [9, 11, 12] and as a new pharmacological target [13, 14]. Several research
3 groups worldwide are involved in the search for new molecular entities to be used as inhibitors of
4 LAT1. The most common approaches used to achieve this goal are: i) *in silico* virtual screening
5 that, however, requires high quality three dimensional structure of the target and ii) *in vitro*
6 screening, generally performed with cell models. Recently, we exploited proteoliposome
7 technology for assaying LAT1 function. With this model, the activity of a membrane protein can be
8 detected in a "clean" system without interferences by other transport or enzymatic systems. Using
9 this technology, a screening of a large group of potential inhibitors with dithiazole- or dithiazine-
10 based structure was performed. Dithiazoles were previously tested on the rat isoform of ASCT2 and
11 some lead molecules were identified exhibiting IC₅₀ from 4 to 10 μM. Interestingly, the
12 hypothesized molecular mechanism of ASCT2 inhibition was based on reaction of dithiazoles with
13 specific Cys residue(s) of the protein, belonging to a CXXC motif of the rat protein [15, 16]. This
14 type of covalent reaction mechanism was exploited for stably inactivating LAT1. The results
15 obtained in the present study led to the identification of potent hLAT1 inhibitors.
16
17
18
19
20
21
22
23
24
25
26
27
28
29
30
31
32
33
34
35
36
37
38

39 **2. Materials and methods**

40 *2.1. Materials*

41 His Trap HP columns and PD-10 columns were purchased from GE Healthcare; radiolabeled amino
42 acids were purchased from ARC (American Radiolabeled Chemicals); all the other reagents are
43 from Sigma-Aldrich.
44
45
46
47
48
49
50

51 *2.2. Synthesis of 1,2,3-dithiazoles 1-55 and 1,2,4-dithiazines 56-59*

52 *2.2.1. General methods and materials*

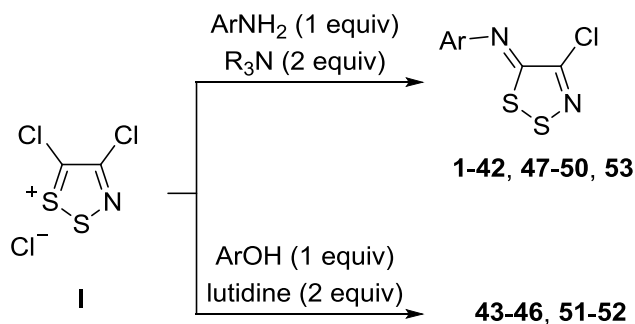
53 Reactions were protected from atmospheric moisture by CaCl₂ drying tubes. Anhydrous Na₂SO₄
54 was used for drying organic extracts, and all volatiles were removed under reduced pressure.
55
56
57
58
59
60
61
62
63
64
65

1 Decomposition points were determined using the TA Instrument DSC Q1000 with samples
2 hermetically sealed in aluminium pans under an argon atmosphere, using heating rates of 5 °C/min.
3
4 UV/vis spectra were obtained using a Shimadzu UV-1601 UV/vis spectrophotometer and
5
6 inflections are identified by the abbreviation “inf”. IR spectra were recorded on a Shimadzu FTIR-
7
8
9 NIR Prestige-21 spectrometer with a Pike Miracle Ge ATR accessory. NMR spectra were recorded
10
11 on a Bruker Avance 500 MHz instrument. Deuterated solvents were used for homonuclear lock and
12
13 internal calibration. MALDI-TOF mass spectra were recorded on a Bruker Autoflex III Smartbeam
14
15 instrument. Elemental analysis was performed on a Perkin Elmer 2400 Series Elemental Analyzer
16
17 by Stephen Boyer of London Metropolitan University.
18
19
20
21

22 2.2.2. Synthesis of 1,2,3-dithiazoles **1-55**

23
24

25 For the preparation of the 1,2,3-dithiazoles, primary aromatic or heteroaromatic amines or alcohols
26
27 were reacted with 4,5-dichloro-1,2,3-dithiazolium chloride (Appel’s salt) I, followed by treatment
28
29 with base (2 equiv) to give the corresponding [(4-chloro-5*H*-1,2,3-dithiazol-5-ylidene)amino]arenes
30
31 or 2-(4-chloro-5*H*-1,2,3-dithiazol-5-ylidene)arene-1(2*H*)-ones **1-53** in moderate to excellent yields
32
33 [17-19] according to the following general procedure: to a stirred suspension of Appel’s salt I (100
34
35 mg, 0.48 mmol) in dichloromethane (4 mL) at *ca.* 20 °C was added the corresponding aminoarene
36
37 or hydroxyarene (0.48 mmol). After 1 h, the appropriate base [*e.g.* Hunig’s base (167 µL, 0.96
38
39 mmol)] was added dropwise to the reaction mixture. After stirring of 2 h the reaction mixture was
40
41 loaded onto silica and purified by dry flash chromatography to afford the corresponding [(4-chloro-
42
43 5*H*-1,2,3-dithiazol-5-ylidene)amino]arene or 2-(4-chloro-5*H*-1,2,3-dithiazol-5-ylidene)arene-1(2*H*)-
44
45
46
47
48
49 one.
50
51
52
53
54
55
56
57
58
59
60
61
62
63
64
65



12 Analytical and spectroscopic data of the 1,2,3-dithiazoles **1-46** and **51-53** have been previously
13 reported [15]. Analytical, physicochemical and spectroscopic data of the newly synthesized 1,2,3-
14 dithiazoles **47-50** are reported below:

15
16
17
18
19
20 *(Z)*-4-Chloro-N-[4-(morpholinomethyl)phenyl]-5H-1,2,3-dithiazol-5-imine (**47**). Yellow oil (66%);
21
22 R_f 0.35 (DCM/Et₂O, 70:30); (found: C, 47.59; H, 4.38; N, 13.01. C₁₃H₁₄ClN₃OS₂ requires C, 47.62;
23
24 H, 4.30; N, 12.82%); λ_{max} (DCM)/nm 240 inf (log ϵ 4.16), 305 (3.44), 378 (3.84), 387 inf (3.83), 410
25
26 inf (3.72); ν_{max}/cm^{-1} 2955w, 2853w and 2805m (alkyl C-H), 1582m, 1533w, 1497m, 1452m,
27
28 1414w, 1395w, 1368w, 1348m, 1333m, 1308w, 1292m, 1263m, 1221m, 1115s, 1069m, 1034m,
29
30 1007m, 914m, 866s, 797m, 764m; δ_H (500 MHz, acetone-*d*₆) 7.49 (1H, d, *J* 8.2), 7.23 (1H, d, *J* 8.4),
31
32 3.63 (2H, t, *J* 4.7), 3.55 (1H, s), 2.44 (3H, br s); δ_C (125 MHz, acetone-*d*₆) 158.8 (s), 150.9 (s), 148.7
33
34 (s), 137.3 (s), 131.4 (d), 120.4 (d), 67.4 (t), 63.3 (t), 54.4 (t); *m/z* (MALDI-TOF) 328 (M⁺+1, 41%),
35
36 326 (M⁺-1, 100).

37
38
39
40
41
42 *(Z)*-4-Chloro-N-[3-(morpholinomethyl)phenyl]-5H-1,2,3-dithiazol-5-imine (**48**). Yellow oil (81%),
43
44 decomp. (DSC) onset: 145.6 °C, peak max: 150.5 °C; R_f 0.48 (DCM/Et₂O, 70:30); (found: C, 47.70;
45
46 H, 4.20; N, 12.94. C₁₃H₁₄ClN₃OS₂ requires C, 47.82; H, 4.30; N, 12.82%); λ_{max} (DCM)/nm 238 inf
47
48 (log ϵ 4.11), 302 (3.35), 377 (3.78), 386 inf (3.77), 409 inf (3.63); ν_{max}/cm^{-1} 2957w, 2855w and
49
50 2805m (alkyl C-H), 1578m, 1524w, 1503w, 1479m, 1454m, 1433m, 1396w, 1368w, 1348m,
51
52 1331m, 1300m, 1281m, 1261m, 1206w, 1163m, 1115s, 1069m, 1034m, 1009m, 908m, 885m, 856s,
53
54 806m, 785m, 758m; δ_H (500 MHz, CDCl₃) 7.41 (1H, dd, *J* 7.7, 7.7), 7.26–7.15 (2H, m), 7.11 (1H, d,
55
56 *J* 7.8), 3.71 (5H, t, *J* 4.5), 3.53 (2H, s), 2.46 (4H, br s); δ_C (125 MHz, CDCl₃) 158.6 (s), 151.2 (s),
57
58
59
60
61
62
63
64
65

1
2 147.9 (s), 140.0 (s), 129.7 (d), 127.3 (d), 120.0 (d), 118.1 (d), 67.0 (t), 63.1 (t), 53.6 (t); *m/z*
3 (MALDI-TOF) 328 (MH⁺, 36%), 326 (M⁺-1, 100), 292 (2), 260 (23), 233 (6), 153 (3).
4

5 *(Z)*-*N*-Benzyl-1-{3-[(4-chloro-5*H*-1,2,3-dithiazol-5-ylidene)amino]phenyl}-*N*-methylmethanamine
6

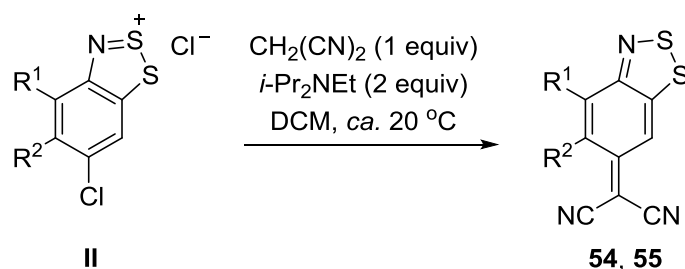
7
8 (**49**). Yellow oil (86%), decomp. (DSC) onset: 145.3 °C, peak max: 154.1 °C; *R*_f 0.47 (DCM/Et₂O,
9 90:10); (found: C, 56.49; H, 4.38; N, 11.73. C₁₇H₁₆ClN₃S₂ requires C, 56.42; H, 4.46; N, 11.61%);
10
11
12 λ_{max} (DCM)/nm 241 inf (log ϵ 4.17), 316 inf (3.45), 378 (3.83), 388 inf (3.82), 409 inf (3.69);
13
14 ν_{max} /cm⁻¹ 3059w and 3026w (aryl C-H), 2833w and 2785m (alkyl C-H), 1578s, 1495m, 1479m,
15
16 1452m, 1415w, 1364m, 1250m, 1159m, 1132m, 1076w, 1026m, 988m, 951w, 934w, 905m, 887m,
17
18 856s, 787m, 760m; δ_{H} (500 MHz, CDCl₃) 7.41 (1H, dd, *J* 7.7, 7.7), 7.40–7.36 (2H, m), 7.33 (2H, dd,
19
20 *J* 7.5, 7.5), 7.30–7.21 (3H, m), 7.11 (1H, d, *J* 8.0), 3.57 (2H, s), 3.56 (2H, s), 2.21 (2H, s); δ_{C} (125
21
22 MHz, CDCl₃) 158.5 (s), 151.2 (s), 148.0 (s), 141.4 (s), 138.9 (s), 129.7 (d), 128.9 (d), 128.3 (d),
23
24 127.1 (d), 127.0 (d), 119.7 (d), 118.0 (d), 61.9 (t), 61.4 (t), 42.2 (q); *m/z* (MALDI-TOF) 362 (MH⁺,
25
26 31%), 360 (M⁺-1, 100), 294 (17), 267 (18), 91 (1).
27
28
29
30
31

32
33 *(Z)*-*N*-Benzyl-1-{4-[(4-chloro-5*H*-1,2,3-dithiazol-5-ylidene)amino]phenyl}-*N*-methylmethanamine
34

35
36 (**50**). Yellow oil (90%), decomp. (DSC) onset: 142.7 °C, peak max: 150.5 °C; *R*_f 0.36 (DCM/Et₂O,
37 70:30); (found: C, 56.35; H, 4.38; N, 11.50. C₁₇H₁₆ClN₃S₂ requires C, 56.42; H, 4.46; N, 11.61%);
38
39
40 λ_{max} (DCM)/nm 242 inf (log ϵ 4.15), 301 (3.49), 388 (3.85), 410 inf (3.65); ν_{max} /cm⁻¹ 3026w (aryl C-
41
42 H), 2920w, 2837w and 2785m (alkyl C-H), 1582m, 1533w, 1497m, 1452m, 1410w, 1366m, 1342w,
43
44 1308w, 1292w, 1265w, 1236m, 1219m, 1171m, 1134m, 1099m, 1024m, 1013m, 901s, 860s, 799w,
45
46 764s; δ_{H} (500 MHz, acetone-*d*₆) 7.56 (2H, d, *J* 7.7), 7.43 (2H, d, *J* 7.2), 7.34 (2H, dd, *J* 7.5, 7.5),
47
48 7.30–7.20 (3H, m), 3.61 (4H, br s), 2.19 (3H, s); δ_{C} (125 MHz, CDCl₃) 157.8 (s), 149.6 (s), 148.1
49
50 (s), 138.8 (s), 137.8 (s), 130.3 (d), 129.0 (d), 128.3 (d), 127.1 (d), 119.5 (d), 61.9 (t), 61.2 (t), 42.2
51
52 (q); *m/z* (MALDI-TOF) 362 (MH⁺, 49%), 360 (M⁺-1, 100), 267 (4), 243 (28), 241 (65), 91 (3).
53
54
55
56
57

58 For the preparation of (6*H*-1,2,3-benzodithiazol-6-ylidene)propanedinitriles, **54** and **55**, substituted
59
60 6-chloro-1,2,3-benzodithiazol-2-ium chlorides **II** (Herz salts) were condensed with malononitrile (1
61
62
63
64
65

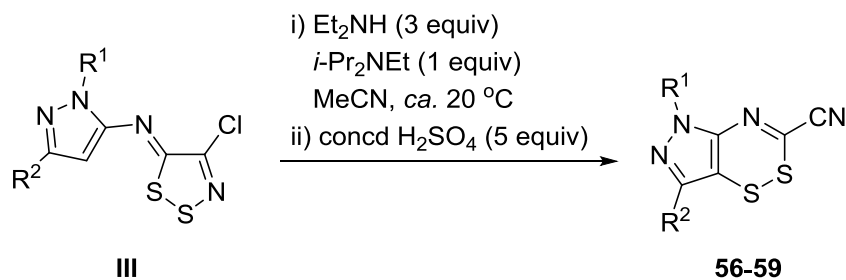
1
2
3
4
5
6
7
8
9
10
11
12
13
14
15
16
17
18
19
20
21
22
23
24
25
26
27
28
29
30
equiv) in the presence of base (2 equiv) according to the following general procedure: To a stirred suspension of the appropriate 6-chloro-1,2,3-benzodithiazol-2-ium chloride **II** (1 mmol) in dichloromethane (25 mL) at *ca.* 20 °C, malononitrile (66 mg, 1 mmol) was added followed by the addition of Hünig's base (348 μ L, 2 mmol). After 1 h the reaction mixture adsorbed onto silica and dry flash chromatography gave the corresponding (6*H*-1,2,3-benzodithiazol-6-ylidene)propanedinitriles **54** or **55**. Analytical and spectroscopic data of the (6*H*-1,2,3-benzodithiazol-6-ylidene)propanedinitriles **54** and **55** have been previously reported [20].



31 32 33 34 35 36 37 38 39 40 41 42 43 44 45 46 47 48 49 50 51 52 53 54 55 56 57 58 59 60 61 62 63 64 65

2.2.3. Synthesis of 1,2,4-dithiazines **56-59**

The synthesis of 1,2,4-dithiazines **56-59** has been recently reported, [21] and involves the reaction of the appropriate (*Z*)-*N*-(4-chloro-5*H*-1,2,3-dithiazol-5-ylidene)-1*H*-pyrazol-5-amine **III** with diethylamine followed by treatment with concd H_2SO_4 according to the following general procedure: To a stirred suspension of the appropriate (*Z*)-*N*-(4-chloro-5*H*-1,2,3-dithiazol-5-ylidene)-1*H*-pyrazol-5-amine (0.2 mmol) in MeCN (4 mL) at *ca.* 20 °C was added Hünig's base (34.5 μ L, 0.2 mmol) followed by diethylamine (63.0 μ L, 0.6 mmol). After complete consumption of the starting material, to the mixture was added in one portion concd H_2SO_4 (55 μ L, 1 mmol). The mixture was stirred for 5 min and then adsorbed onto silica and chromatographed to give the corresponding 5*H*-pyrazolo[3,4-*e*][1,2,4]dithiazine-3-carbonitrile. Analytical and spectroscopic data of the 1,2,4-dithiazines **56-59** have been previously reported [21].



13 **2.3. Purification of hLAT1**

14
15
16 hLAT1 wild type and mutants C335A, C407A and C335A/C407A over-expressed in *E. Coli* were
17 purified as previously described [3]. After cell lysate solubilisation and centrifugation (12,000 g, 10
18 min, 4 °C), the purification was performed using ÄKTA start. In particular, the supernatant was
19 applied on a His Trap HP column (5 ml Ni Sepharose) equilibrated with 10 mL buffer (20 mM Tris
20 HCl pH 8.0, 10% glycerol, 200 mM NaCl, 0.1% sarkosyl, and DTE 2 mM) while the protein was
21 eluted with the same buffer plus 400 mM imidazole. Desalt of 2.5 mL of the purified protein was
22 than performed using a PD-10 column.
23
24
25
26
27
28
29
30
31
32

33
34 **2.4. Reconstitution of the purified hLAT1**

35
36
37 The purified hLAT1 was reconstituted by removing detergent from mixed micelles containing
38 detergent, protein and phospholipids using batch wise method as previously described [3]. The
39 initial mixture contained: 4 µg of purified protein, 100 µL of 10% C₁₂E₈, 100 µL of 10% egg yolk
40 phospholipids (*w/v*) in the form of liposomes prepared as previously described [22], 20 mM Tris
41 HCl pH 7.5 and 10 mM L-His in a final volume of 700 µL.
42
43
44
45
46
47
48
49

50 **2.5. Transport measurements**

51
52
53 To remove the external substrate, 600 µL of proteoliposomes were passed through a Sephadex G-75
54 column (0.7 cm diameter × 15 cm height) pre-equilibrated with 20 mM Tris HCl pH 7.5 and
55 sucrose at an appropriate concentration to balance internal osmolarity. Transport was initiated by
56 adding 5 µM [³H]His to proteoliposomes and stopped by a mixture of 100 µM BCH and 1.5 µM
57
58
59
60
61
62
63
64
65

1 HgCl₂. In controls, the mixture of inhibitors was added at time zero according to the inhibitor stop
2 method [23]. 100 μL of proteoliposomes were passed through a Sephadex G-75 column (0.6 cm
3 diameter × 8 cm height) at the end of the transport assay, to separate the external from the internal
4 radioactivity. Proteoliposomes were eluted with 1 mL 50 mM NaCl in 4 mL scintillation mixture
5 and counted. For [³H]His uptake analysis, experimental values were corrected by subtracting
6 controls. Initial transport rate was measured by stopping the reaction after 15 min for wild type
7 protein and after 30 min for Cys mutants, *i.e.*, within the initial linear range of [³H]His uptake in
8 proteoliposomes. Grafit 5.0.13 software was used to calculate kinetic parameters and derive IC₅₀
9 values in inhibition assays. Protein concentration was estimated by Chemidoc imaging system to
10 calculate the hLAT1 specific activity [24].
11
12
13
14
15
16
17
18
19
20
21
22
23
24

25 2.6. Cell culture

26
27 HEK293 and SiHa cells, at late passage and kindly provided by Dr. Massimo Tommasino Infection
28 and Cancer Biology group (IARC/CIRC- WHO/OMS), were maintained in Dulbecco's Modified
29 Eagle Medium (DMEM) supplemented with 10% (*v/v*) fetal bovine serum (FBS), 1 mM glutamine
30 and 1 mM sodium pyruvate and Pen/Strep as antibiotics. Cells were grown on 10 cm² plates at 37
31 °C in a humidified incubator and a 5% CO₂ atmosphere.
32
33
34
35
36
37
38
39
40

41 2.7. Transport measurement in HEK293 cells

42
43 pCDNA3hLAT1-HA was obtained by subcloning the cDNA of hLAT1 between BamHIII and XhoI
44 restriction site into pCDNA3 mammalian expression vector. The HA tag was added by two
45 sequential PCR reaction using the reverse 1
46 ATCTGGAACATCGTATGGGTATGTCTCCTGGGGGACCAC, then the reverse 2
47 CGGTCTCGAGCTAAGCGTAATCTGGAACATCGTATGGGTA and a single forward
48 CGCGGATCCACCATGGCGGGTGCGGGCCCGAAG. The construct was verified by DNA
49 sequencing. HEK293 cells were seeded onto 10 cm² plates and cultured using standard culturing
50 conditions until they reached 80% confluence. Cells were transfected with Polyjet (Signagen
51
52
53
54
55
56
57
58
59
60
61
62
63
64
65

Laboratories) transfection reagent according to the manufacturer's procedures with 5 μg of pCDNA3hLAT1-HA or empty vector. After 24 h, empty vector or hLAT1 expressing cells were seeded onto 12 well plates and used for transport assay of L- $[\text{}^3\text{H}]\text{His}$. Cells were rinsed twice with warm transport buffer: 20 mM Tris HCl pH 7.4 and 5 mM glucose. Radiolabeled 5 μM $[\text{}^3\text{H}]\text{His}$ was added and the transport reaction was terminated after 1 min by discarding the uptake buffer and rinsing the cells three times with the same ice-cold transport buffer (0.5 mL per well per rinse) plus 10 mM BCH. Cells from each well were solubilized in 500 μL of 1% TX-100 solution. Cell extracts were counted for radioactivity (400 μL). The remaining 100 μL in each well were used for protein concentration assay. Specific His-transport was evaluated by subtracting the transport values of cells transfected with hLAT1 to those transfected with empty vector. To verify hLAT1 overexpression, western blot analysis was conducted on cell lysates harboring or not hLAT1-HA. The protein was immuno-detected incubating membrane with anti-HA (Sigma Aldrich) antibody 1:1000 overnight at 4 $^{\circ}\text{C}$. As loading control 1:5000 anti-Actin (Sigma Aldrich) was used 1 h at room temperature. The reactions were detected by Electro Chemi Luminescence (ECL) assay after 1 h incubation at room temperature with secondary antibody anti-mouse (Cell Signaling) 1:5000.

2.8. Cell viability

SiHa cells were seeded onto 6 well plates and cultured using standard culturing conditions until they reached 70% confluence. Cells were treated with 10 and 100 μM of dithiazole inhibitors as indicated in the figure legends. Cell viability were followed for 24 and 48 h and pictures were taken.

2.9. Computational studies

Outward-open hLAT1 structure was obtained by comparative modeling, using the AdiC crystallographic structure (RCSB PDB code: 3OB6) as a template [25]

Tested compounds were drawn and energy minimized by the Molecular Operating Environment (MOE) Builder, with the Amber10:EHT force field. Since 1,2,3-dithiazoles can react with

1 nucleophile compounds, such as C335 and C407, the MOE Dock program was used with the
2 covalent feature.
3

4 The top-scoring poses from the docking procedure were refined by using the MOE QuickPrep
5 procedure aimed at refining the complex before calculating the approximate binding free energy via
6 the GBVI/WSA dG empirical scoring function [26].
7
8
9

10 2.10. Statistical analysis

11 Data points of each experiments derived from samples in triplicates. Threshold for statistical
12 significance (P value) was fixed at 0.01 according to Student's two tailed unpaired T-test. Data
13 reported in Table 1 have been obtained from two experiments for a preliminary screening of the
14 compounds.
15
16
17
18
19
20
21
22
23
24
25
26
27

28 3. Results

29 3.1. Inhibition of the hLAT1 transporter by 1,2,3-dithiazoles 1-55 and 1,2,4-dithiazines 56-59

30 Title compounds 1-59 (Table 1) were prepared and tested as inhibitors of hLAT1. Transport activity
31 was assayed in proteoliposomes as [³H]His_{ex}/His_{in} antiport. Results of this preliminary screening,
32 performed at 100 μM of each compound, are reported in Table 1 as percent of inhibition. The
33 concentration used was about three times the threshold fixed for significant xenobiotic/protein
34 interactions [27]. Several compounds triggered virtually complete inhibition, *i.e.* >90% (Table 1,
35 compounds 5, 10, 11, 12, 16, 17, 19 and 59); the other tested molecules showed a variable extent of
36 inhibition ranging from 0 to 89%. No effect was exerted by DMSO used to solubilize the
37 compounds, demonstrating that the inhibition could be ascribed exclusively to the compounds.
38
39
40
41
42
43
44
45
46
47
48
49
50
51
52
53

54 3.2. Dose-response analysis

55 The compounds showing inhibition higher than 90% at 100 μM were selected for dose-response
56 analyses.
57
58
59
60
61
62
63
64
65

1 In these experiments, the rate of the [³H]His/His antiport was determined in the presence of
2 increasing concentrations of the inhibitors (Fig. 1). As expected, all the selected compounds led to a
3 strong and complete inhibition with IC₅₀ values of: 0.98 ± 0.10, 1.33 ± 0.33, 1.62 ± 0.43, 2.10 ±
4 0.58, 1.62 ± 0.30, 0.89 ± 0.33, 1.87 ± 0.09 and 5.2 ± 0.11 μM for compounds **5**, **10**, **11**, **12**, **16**, **17**,
5
6
7
8
9
10 **19** and **59**, respectively (Fig. 1).

11 12 3.3. Molecular mechanism of interaction/inhibition

13
14
15 Dithiazoles and dithiazines are expected to interact with the protein through formation of mixed
16 disulfide/trisulfide as previously reported ([15, 28, 29] and see Fig. 2). Human LAT1 harbours 12
17 Cys residues in its structure; thus, a strategy for assessing the possible reaction with thiol residues
18 was adopted (Fig. 3): proteoliposomes were treated or not with the two most potent inhibitors, *i.e.*
19
20
21
22
23
24
25
26
27
28
29
30
31
32
33
34
35
36
37
38
39
40
41
42
43
44
45
46
47
48
49
50
51
52
53
54
55
56
57
58
59
60
61
62
63
64
65
66
67
68
69
70
71
72
73
74
75
76
77
78
79
80
81
82
83
84
85
86
87
88
89
90
91
92
93
94
95
96
97
98
99
100
101
102
103
104
105
106
107
108
109
110
111
112
113
114
115
116
117
118
119
120
121
122
123
124
125
126
127
128
129
130
131
132
133
134
135
136
137
138
139
140
141
142
143
144
145
146
147
148
149
150
151
152
153
154
155
156
157
158
159
160
161
162
163
164
165
166
167
168
169
170
171
172
173
174
175
176
177
178
179
180
181
182
183
184
185
186
187
188
189
190
191
192
193
194
195
196
197
198
199
200
201
202
203
204
205
206
207
208
209
210
211
212
213
214
215
216
217
218
219
220
221
222
223
224
225
226
227
228
229
230
231
232
233
234
235
236
237
238
239
240
241
242
243
244
245
246
247
248
249
250
251
252
253
254
255
256
257
258
259
260
261
262
263
264
265
266
267
268
269
270
271
272
273
274
275
276
277
278
279
280
281
282
283
284
285
286
287
288
289
290
291
292
293
294
295
296
297
298
299
300
301
302
303
304
305
306
307
308
309
310
311
312
313
314
315
316
317
318
319
320
321
322
323
324
325
326
327
328
329
330
331
332
333
334
335
336
337
338
339
340
341
342
343
344
345
346
347
348
349
350
351
352
353
354
355
356
357
358
359
360
361
362
363
364
365
366
367
368
369
370
371
372
373
374
375
376
377
378
379
380
381
382
383
384
385
386
387
388
389
390
391
392
393
394
395
396
397
398
399
400
401
402
403
404
405
406
407
408
409
410
411
412
413
414
415
416
417
418
419
420
421
422
423
424
425
426
427
428
429
430
431
432
433
434
435
436
437
438
439
440
441
442
443
444
445
446
447
448
449
450
451
452
453
454
455
456
457
458
459
460
461
462
463
464
465
466
467
468
469
470
471
472
473
474
475
476
477
478
479
480
481
482
483
484
485
486
487
488
489
490
491
492
493
494
495
496
497
498
499
500
501
502
503
504
505
506
507
508
509
510
511
512
513
514
515
516
517
518
519
520
521
522
523
524
525
526
527
528
529
530
531
532
533
534
535
536
537
538
539
540
541
542
543
544
545
546
547
548
549
550
551
552
553
554
555
556
557
558
559
560
561
562
563
564
565
566
567
568
569
570
571
572
573
574
575
576
577
578
579
580
581
582
583
584
585
586
587
588
589
590
591
592
593
594
595
596
597
598
599
600
601
602
603
604
605
606
607
608
609
610
611
612
613
614
615
616
617
618
619
620
621
622
623
624
625
626
627
628
629
630
631
632
633
634
635
636
637
638
639
640
641
642
643
644
645
646
647
648
649
650
651
652
653
654
655
656
657
658
659
660
661
662
663
664
665
666
667
668
669
670
671
672
673
674
675
676
677
678
679
680
681
682
683
684
685
686
687
688
689
690
691
692
693
694
695
696
697
698
699
700
701
702
703
704
705
706
707
708
709
710
711
712
713
714
715
716
717
718
719
720
721
722
723
724
725
726
727
728
729
730
731
732
733
734
735
736
737
738
739
740
741
742
743
744
745
746
747
748
749
750
751
752
753
754
755
756
757
758
759
760
761
762
763
764
765
766
767
768
769
770
771
772
773
774
775
776
777
778
779
780
781
782
783
784
785
786
787
788
789
790
791
792
793
794
795
796
797
798
799
800
801
802
803
804
805
806
807
808
809
810
811
812
813
814
815
816
817
818
819
820
821
822
823
824
825
826
827
828
829
830
831
832
833
834
835
836
837
838
839
840
841
842
843
844
845
846
847
848
849
850
851
852
853
854
855
856
857
858
859
860
861
862
863
864
865
866
867
868
869
870
871
872
873
874
875
876
877
878
879
880
881
882
883
884
885
886
887
888
889
890
891
892
893
894
895
896
897
898
899
900
901
902
903
904
905
906
907
908
909
910
911
912
913
914
915
916
917
918
919
920
921
922
923
924
925
926
927
928
929
930
931
932
933
934
935
936
937
938
939
940
941
942
943
944
945
946
947
948
949
950
951
952
953
954
955
956
957
958
959
960
961
962
963
964
965
966
967
968
969
970
971
972
973
974
975
976
977
978
979
980
981
982
983
984
985
986
987
988
989
990
991
992
993
994
995
996
997
998
999
1000

53 3.4. Kinetics of inhibition

54
55
56 To gain further insights into the molecular mechanism of action, inhibition kinetics was
57 investigated. Experiments were conducted by studying the dependence of transport rate on His
58 concentration in the presence of the compounds **5** and **17** used at concentrations close to their IC₅₀
59
60
61
62
63
64
65

1
2
3
4
5
6
7
8
9
10
11
12
13
14
15
16
17
18
19
20
21
22
23
24
25
26
27
28
29
30
31
32
33
34
35
36
37
38
39
40
41
42
43
44
45
46
47
48
49
50
51
52
53
54
55
56
57
58
59
60
61
62
63
64
65

(Fig. 5). The data were analysed by double reciprocal plots, according to Lineweaver-Burk, from which straight line patterns intersecting on or close to the x -axis was found. Mixed or non-competitive inhibition was found for compound **5** (Fig. 5 A). Mixed inhibition was found for compound **17** (Fig. 5 B). The half saturation constant K_i , calculated from the experiments were $0.76 \pm 0.27 \mu\text{M}$ and $1.13 \pm 0.41 \mu\text{M}$ for compounds **5** and **17**, respectively (Fig. 5 A-B). The potential protection of inhibition by substrate was also tested. Pre-incubation of proteoliposomes with His at concentrations up to 10 mM was performed prior to dithiazoles. No protection by His was observed with compound **5** (Fig. 5 C), in agreement with the covalent mechanism, *i.e.* non-competitive, of the inhibition described.

3.5. Homology model and effects on LAT1 mutants

The reactivity of dithiazoles towards SH groups of the protein allowed to hypothesize the involvement of one or more Cys residues of the protein as the nucleophilic group attacking the cyclic disulfide bond on the inhibitor. The availability of 3D homology model [3] allowed us to perform covalent docking simulations both on C335 and C407 for compounds **5** and **17**, showing that both these compounds can bind C407 (covalent docking score and approximate binding free energy for compound **5**: -4.8 kcal/mol and -21.4 kcal/mol, respectively; covalent docking score and approximate binding free energy for compound **17**: -3.1 kcal/mol and -14.6 kcal/mol, respectively) (Fig. 6), whereas both the tested compounds cannot covalently bind C335; moreover, compound **51** has been used as negative control of docking (covalent docking score for compound **52**, 125.6 kcal/mol) being a poor inhibitor of LAT1 (Table 1).

Interestingly, the identified residue was C407 located in the substrate binding site as previously demonstrated [3]. Thus, the C407A mutant was used for dose-response analyses performed on compound **5**. This was chosen due to its higher affinity (K_i value), confirmed by the good covalent docking score and approximate binding free energy obtained in silico. The calculated IC_{50} of the C407 mutant was $3.76 \pm 0.28 \mu\text{M}$, *i.e.* four times higher than that of wild type (Fig. 7A). The

1 substrate binding site includes also C335 for which docking analysis predicted no interaction with
2 both compounds **5** and **17**. Indeed, IC₅₀ of C335A mutant derived from dose-response analysis on
3 compound **5** was 1.32 ± 0.16 μM (Fig. 7B), *i.e.* similar to that of wild type (Fig. 1A). To further
4 ascertain the exclusive role of C407, the IC₅₀ was calculated also for the double mutant
5 C335A/C407A (Fig. 7C). In this case, a value of 4.60 ± 0.39 μM was obtained, similar to that of the
6 single mutant C407A.
7
8
9

10 3.6. Effects on intact cells 11 12 13 14

15 Given the strong inhibitory effect of compound **5**, inhibition experiments were performed on intact
16 HEK293 cells transiently transfected with hLAT1-HA. Fig. 8A demonstrates the actual over
17 expression of hLAT1 detected by an anti-HA antibody as control. [³H]His uptake was measured in
18 the presence or absence of compound **5** (Fig. 8B) at a concentration corresponding to its IC₅₀ in
19 proteoliposomes (Fig. 1A). Transport in HEK293 cells was inhibited by about 50% confirming that
20 the compound inhibits hLAT1 in intact cells at the same extent as in proteoliposomes. To gain
21 further insight on the biological effects of inhibitors, cell viability was tested. In this case, SiHa cell
22 line was used since these cells harbor a detectable level of endogenous LAT1 [30]. The experiment
23 was conducted by monitoring cell morphology 24 and 48 h after addition of increasing
24 concentrations of the most active compounds **5** and **17** or the negative control compound **51** that
25 showed <37% inhibition in proteoliposomes (Table 1); DMSO was added to control cells, *i.e.*, in
26 the absence of inhibitor (Fig. 9). Interestingly, the compounds with the lowest IC₅₀ were very
27 effective in inducing apparent cell death triggering significant reduction of cell numbers together
28 with evident changes in cell morphology. The effects were more pronounced after 48 h.
29 Interestingly, after washing out the compounds, cell viability was still impaired. Compound **51** was
30 used as specificity control being one of the compounds with the lowest inhibitory effects on LAT1.
31 Notably, the compound did not cause cell death highlighting the specificity of the tested dithiazoles
32 with respect to hLAT1 activity.
33
34
35
36
37
38
39
40
41
42
43
44
45
46
47
48
49
50
51
52
53
54
55
56
57
58
59
60
61
62
63
64
65

4. Discussion

In the last 10 years, more than 200 papers appeared on Pubmed database ["LAT1" (or aliases) and "cancer" (or aliases) as query in Title/Abstract] dealing with LAT1 over-expression in several human cancers. On this basis, the transporter became acknowledged as a new pharmacological target for cancer therapy. LAT1 has been also exploited for delivery of pharmacological compounds which mimic its substrates as proposed in the pro-drug approach [31]. Proteoliposomes reconstituted with hLAT1 have been used in the present work as the main experimental model for screening of inhibitors due to its intrinsic simplicity being not affected by other transport activities. Data on inhibitors have been then confirmed on experimental models closer to the *in vivo* conditions.

The task of designing good ligands/inhibitors for LAT1 is challenging, as for most membrane transporters, owing to the absence of its 3D crystallographic structure. Indeed, LAT1 structures were derived, so far, by homology modeling on the basis of the arginine/agmatine transporter, *i.e.* AdiC from *E. coli* [3, 25, 32-34], sharing a relatively low sequence identity with hLAT1. From these models, some features of LAT1 substrate binding site were predicted and exploited for designing not transported substrate-mimicking molecules, with the aim of finding potent competitive inhibitors [4, 35-38], following a strategy firstly used for designing inhibitors of the ASCT2 amino acid transporter [39]. A limitation of this type of inhibitors resides in the competition exerted by endogenous amino acid substrates which have plasma concentrations higher than the K_m for transporters [10, 40]. In this case, inhibitors can be displaced from the transporter site leading to only transient or inefficient effects [35]. Herein, an alternative strategy has been attempted taking into account the information recently obtained on structure-function relationships of LAT1 substrate site [3]. Indeed, we exploited the presence of Cys residues in the substrate binding site of the protein to obtain, on the one hand, a more potent inhibition in terms of affinity, on the other hand, an irreversible inhibition mechanism to chemically knocking-out the transporter. Thus, a number of

1 electrophilic molecules has been tested, likely reacting covalently with the thiolate group of a Cys,
2 that are dithiazoles and dithiazines, known for their antibacterial, antifungal, herbicidal and
3 anticancer effects [41-49]. Noteworthy, some of these compounds were previously described as
4 covalent inhibitors of rat ASCT2 transporter [15].
5
6
7

8
9 The variety of chemical substituents on the 1,2,3-dithiazole and to a lower extent on the 1,2,4-
10 dithiazine rings allowed us to discover a number of compounds with a very high affinity for LAT1
11 showing the lowest IC₅₀ achieved so far, *i.e.*, half the previous lowest value [36]. Regarding
12 reactivity of the compounds, the S2 atom of the disulfide motif (Fig. 2), would represent the
13 preferred electrophilic site for the attack by a thiolate of a Cys residue of the protein but the
14 nucleophilic attack on S1 cannot be excluded. The reaction mechanism may therefore occur via the
15 formation of mixed di- or trisulfides, as previously suggested for the reaction of the same
16 compounds with another amino acid transporter [15]. The mixed disulfide mechanism has been
17 adopted (Fig. 2) for docking calculations since this is the most widely occurring mechanism *in vivo*.
18 That inhibition was due to covalent interaction was demonstrated herein for the most effective
19 compounds **5** and **17**. Three different strategies were adopted to identify the mechanism of
20 inhibition and the Cys residue targeted by these compounds. Firstly, the significant activity
21 recovery induced by the thiol reducing agent DTE indicated involvement of Cys residue(s) in the
22 covalent interaction with compounds. However, in the case of compound **17**, DTE did not allow
23 100% recovery of LAT1 transport activity probably because of additional hydrophobic interactions
24 independent from thiol reactivity. Secondly, the kinetics showed a non-competitive and mixed type
25 inhibition for both compounds **5** and **17** that supported the covalent interaction with LAT1. In line
26 with these experimental data, C407 was definitively identified as the target of compound **5** by site-
27 directed mutagenesis.
28
29
30
31
32
33
34
35
36
37
38
39
40
41
42
43
44
45
46
47
48
49
50
51
52
53
54

55 C407, being located in the substrate binding site may be easily blocked by mixed sulfide formation
56 triggering the competitive component of the inhibition. Accordingly, the pre-incubation of
57
58
59
60
61
62
63
64
65

1 reconstituted proteoliposomes with excess of substrate did not alter the inhibition potency by
2 compounds **5**.

3
4 Some information on SAR trends can be obtained from the IC₅₀ of the eight most active compounds
5
6 and from the % of inhibition by all the others. It seems likely that electron withdrawal substituents
7
8 on the phenyl ring facilitate the interaction/binding to the protein resulting in a higher inhibitory
9
10 effect, with the exception of compound **2**. In contrast, electron-donating and bulky substituents,
11
12 along with polycyclic compounds, are in general less effective in blocking LAT1 transport activity.
13
14 The pyrid-2-yl *sp*² nitrogen lone pair of dithiazoles **26-29**, **32** and **33** donates electron density into
15
16 the antibonding S-S bond of the dithiazole and this raises the electron density of the ring, making it
17
18 less prone to thiophilic attack. This explains the sudden drop in activity of such dithiazoles while,
19
20 interestingly, the introduction of electron withdrawing groups (as the cyano group in **27**) restores
21
22 some activity. This electronic effect was recently detected in the evaluation of 1,2,3-dithiazoles
23
24 reactivity [29].
25
26
27
28
29
30

31 Interestingly, the strategy adopted in this work responded also to the 3R requirement for animal
32
33 testing: Replace, Reduce, Refine. In fact, out of 59 compounds 8 hits were identified and, among
34
35 them, 2 lead compounds were chosen for a deep investigation. Only at the very end of the
36
37 screening, the selected compounds, for which the molecular mechanism of action was deciphered in
38
39 proteoliposomes, were used to verify effects on cell viability. Taken together, the collected results
40
41 defined, with relatively low cost and no animal experimentation, the molecular scaffold that could
42
43 be used for designing potential drugs to be used in more advanced pre-clinical trials.
44
45
46
47
48
49

50 51 **Conflicts of interest**

52 The authors declared that they have no competing interests.
53
54
55

56 **Acknowledgements**

57 This work was supported by Ministry of Instruction University and Research (MIUR)-Italy, by a
58
59 grant from PON-ricerca e competitività 2007–2013 (PON project 01_00937: “Modelli sperimentali
60
61
62
63
64
65

1 biotecnologici integrati per la produzione ed il monitoraggio di molecole di interesse per la salute
2 dell'uomo"). PK and MK thank the Cyprus Research Promotion Foundation (Grant:
3 NEKYP/0308/02) and the following organizations and companies in Cyprus for generous donations
4 of chemicals and glassware: the State General Laboratory, the Agricultural Research Institute, the
5 Ministry of Agriculture, MedoChemie Ltd, Medisell Ltd and Biotronics Ltd. Furthermore, we thank
6
7 the A. G. Leventis Foundation for helping to establish the NMR facility at the University of Cyprus.
8
9
10
11
12
13
14

15 References

- 16
17
18 [1] D. Fotiadis, Y. Kanai, M. Palacin, The SLC3 and SLC7 families of amino acid transporters, *Molecular*
19 *aspects of medicine* 34(2-3) (2013) 139-58.
20 [2] J. Fort, L.R. de la Ballina, H.E. Burghardt, C. Ferrer-Costa, J. Turnay, C. Ferrer-Orta, I. Uson, A.
21 Zorzano, J. Fernandez-Recio, M. Orozco, M.A. Lizarbe, I. Fita, M. Palacin, The structure of human 4F2hc
22 ectodomain provides a model for homodimerization and electrostatic interaction with plasma membrane, *The*
23 *Journal of biological chemistry* 282(43) (2007) 31444-52.
24 [3] L. Napolitano, M. Galluccio, M. Scalise, C. Parravicini, L. Palazzolo, I. Eberini, C. Indiveri, Novel
25 insights into the transport mechanism of the human amino acid transporter LAT1 (SLC7A5). Probing critical
26 residues for substrate translocation, *Biochimica et biophysica acta* 1861(4) (2017) 727-736.
27 [4] E.G. Geier, A. Schlessinger, H. Fan, J.E. Gable, J.J. Irwin, A. Sali, K.M. Giacomini, Structure-based
28 ligand discovery for the Large-neutral Amino Acid Transporter 1, LAT-1, *Proceedings of the National*
29 *Academy of Sciences of the United States of America* 110(14) (2013) 5480-5.
30 [5] D.C. Tarlunganu, E. Deliu, C.P. Dotter, M. Kara, P.C. Janiesch, M. Scalise, M. Galluccio, M. Tesulov,
31 E. Morelli, F.M. Sonmez, K. Bilguvar, R. Ohgaki, Y. Kanai, A. Johansen, S. Esharif, T. Ben-Omran, M.
32 Topcu, A. Schlessinger, C. Indiveri, K.E. Duncan, A.O. Caglayan, M. Gunel, J.G. Gleeson, G. Novarino,
33 Impaired Amino Acid Transport at the Blood Brain Barrier Is a Cause of Autism Spectrum Disorder, *Cell*
34 167(6) (2016) 1481-1494 e18.
35 [6] R. Milkereit, A. Persaud, L. Vanoaica, A. Guetg, F. Verrey, D. Rotin, LAPTM4b recruits the LAT1-
36 4F2hc Leu transporter to lysosomes and promotes mTORC1 activation, *Nature communications* 6 (2015)
37 7250.
38 [7] M. Rebsamen, L. Pochini, T. Stasyk, M.E. de Araujo, M. Galluccio, R.K. Kandasamy, B. Snijder, A.
39 Fauster, E.L. Rudashevskaya, M. Bruckner, S. Scorzoni, P.A. Filipek, K.V. Huber, J.W. Bigenzahn, L.X.
40 Heinz, C. Kraft, K.L. Bennett, C. Indiveri, L.A. Huber, G. Superti-Furga, SLC38A9 is a component of the
41 lysosomal amino acid sensing machinery that controls mTORC1, *Nature* 519(7544) (2015) 477-81.
42 [8] S. Wang, Z.Y. Tsun, R.L. Wolfson, K. Shen, G.A. Wyant, M.E. Plovanich, E.D. Yuan, T.D. Jones, L.
43 Chantranupong, W. Comb, T. Wang, L. Bar-Peled, R. Zoncu, C. Straub, C. Kim, J. Park, B.L. Sabatini, D.M.
44 Sabatini, *Metabolism. Lysosomal amino acid transporter SLC38A9 signals arginine sufficiency to mTORC1,*
45 *Science* 347(6218) (2015) 188-94.
46 [9] Y.D. Bhutia, E. Babu, S. Ramachandran, V. Ganapathy, Amino Acid transporters in cancer and their
47 relevance to "glutamine addiction": novel targets for the design of a new class of anticancer drugs, *Cancer*
48 *research* 75(9) (2015) 1782-8.
49 [10] M. Scalise, L. Pochini, M. Galluccio, C. Indiveri, Glutamine transport. From energy supply to sensing
50 and beyond, *Biochimica et biophysica acta* 1857(8) (2016) 1147-57.
51 [11] B.C. Fuchs, B.P. Bode, Amino acid transporters ASCT2 and LAT1 in cancer: partners in crime?,
52 *Seminars in cancer biology* 15(4) (2005) 254-66.
53 [12] Y. Zhao, L. Wang, J. Pan, The role of L-type amino acid transporter 1 in human tumors, *Intractable &*
54 *rare diseases research* 4(4) (2015) 165-9.
55 [13] V. Ganapathy, M. Thangaraju, P.D. Prasad, Nutrient transporters in cancer: relevance to Warburg
56 hypothesis and beyond, *Pharmacology & therapeutics* 121(1) (2009) 29-40.
57
58
59
60
61
62
63
64
65

- [14] L. Yang, T. Moss, L.S. Mangala, J. Marini, H. Zhao, S. Wahlig, G. Armaiz-Pena, D. Jiang, A. Achreja, J. Win, R. Roopaimoole, C. Rodriguez-Aguayo, I. Mercado-Urbe, G. Lopez-Berestein, J. Liu, T. Tsukamoto, A.K. Sood, P.T. Ram, D. Nagrath, Metabolic shifts toward glutamine regulate tumor growth, invasion and bioenergetics in ovarian cancer, *Molecular systems biology* 10 (2014) 728.
- [15] F. Oppedisano, M. Catto, P.A. Koutentis, O. Nicolotti, L. Pochini, M. Koyioni, A. Introcaso, S.S. Michaelidou, A. Carotti, C. Indiveri, Inactivation of the glutamine/amino acid transporter ASCT2 by 1,2,3-dithiazoles: proteoliposomes as a tool to gain insights in the molecular mechanism of action and of antitumor activity, *Toxicology and applied pharmacology* 265(1) (2012) 93-102.
- [16] L. Pochini, M. Scalise, M. Galluccio, C. Indiveri, Membrane transporters for the special amino acid glutamine: structure/function relationships and relevance to human health, *Frontiers in chemistry* 2 (2014) 61.
- [17] J.H. Appel R., Siray M., Knoch F., Synthesis and reactions of 4,5-dichloro-1,2,3-dithiazolium chloride, *Chem. Ber. Recl.* 118 (1985) 1632–1643.
- [18] R.O.A. English R.F., Rees C.W., Vlasova O.G., Conversion of imino-1,2,3-dithiazoles into 2-cyanobenzothiazoles, cyanoimidoyl chlorides and diatomic sulfur, *J. Chem. Soc. Perkin Trans. 1* (1997) 201-205.
- [19] P.A. Koutentis, M. Koyioni, S.S. Michaelidou, Synthesis of [(4-chloro-5H-1,2,3-dithiazol-5-ylidene)amino]azines, *Molecules* 16(11) (2011) 8992-9002.
- [20] P. A. Koutentis, C.W. Rees, Reaction of Herz salts with malononitrile: A general route to (6H-1,2,3-benzodithiazol-6-ylidene)malononitriles, *J. Chem. Soc. Perkin Trans. 1* (2002) 315-319.
- [21] M. Koyioni, M. Manoli, P.A. Koutentis, Synthesis of fused 1,2,4-dithiazines and 1,2,3,5-trithiazepines, *The Journal of organic chemistry* 79(20) (2014) 9717-27.
- [22] C. Indiveri, G. Prezioso, T. Dierks, R. Kramer, F. Palmieri, Kinetic characterization of the reconstituted dicarboxylate carrier from mitochondria: a four-binding-site sequential transport system, *Biochimica et biophysica acta* 1143(3) (1993) 310-8.
- [23] F. Palmieri, C. Indiveri, F. Bisaccia, V. Iacobazzi, Mitochondrial metabolite carrier proteins: purification, reconstitution, and transport studies, *Methods in enzymology* 260 (1995) 349-69.
- [24] E.M. Torchetti, C. Brizio, M. Colella, M. Galluccio, T.A. Giancaspero, C. Indiveri, M. Roberti, M. Barile, Mitochondrial localization of human FAD synthetase isoform 1, *Mitochondrion* 10(3) (2010) 263-73.
- [25] L. Kowalczyk, M. Ratera, A. Paladino, P. Bartoccioni, E. Errasti-Murugarren, E. Valencia, G. Portella, S. Bial, A. Zorzano, I. Fita, M. Orozco, X. Carpena, J.L. Vazquez-Ibar, M. Palacin, Molecular basis of substrate-induced permeation by an amino acid antiporter, *Proceedings of the National Academy of Sciences of the United States of America* 108(10) (2011) 3935-40.
- [26] M. Naim, S. Bhat, K.N. Rankin, S. Dennis, S.F. Chowdhury, I. Siddiqi, P. Drabik, T. Sulea, C.I. Bayly, A. Jakalian, E.O. Purisima, Solvated interaction energy (SIE) for scoring protein-ligand binding affinities. 1. Exploring the parameter space, *Journal of chemical information and modeling* 47(1) (2007) 122-33.
- [27] E. Lounkine, M.J. Keiser, S. Whitebread, D. Mikhailov, J. Hamon, J.L. Jenkins, P. Lavan, E. Weber, A.K. Doak, S. Cote, B.K. Shoichet, L. Urban, Large-scale prediction and testing of drug activity on side-effect targets, *Nature* 486(7403) (2012) 361-7.
- [28] A. Gupta, P. Mishra, S.K. Kashaw, V. Jatav, Synthesis, Anticonvulsant, Antimicrobial and Analgesic activity of Novel 1,2,4-Dithiazoles, *Indian journal of pharmaceutical sciences* 70(4) (2008) 535-8.
- [29] M. Koyioni, M. Manoli, P.A. Koutentis, The Reaction of DABCO with 4-Chloro-5H-1,2,3-dithiazoles: Synthesis and Chemistry of 4-[N-(2-Chloroethyl)piperazin-1-yl]-5H-1,2,3-dithiazoles, *The Journal of organic chemistry* 81(2) (2016) 615-31.
- [30] L. Napolitano, M. Scalise, M. Galluccio, L. Pochini, L.M. Albanese, C. Indiveri, LAT1 is the transport competent unit of the LAT1/CD98 heterodimeric amino acid transporter, *The international journal of biochemistry & cell biology* 67 (2015) 25-33.
- [31] L. Peura, K. Malmioja, K. Laine, J. Leppanen, M. Gynther, A. Isotalo, J. Rautio, Large amino acid transporter 1 (LAT1) prodrugs of valproic acid: new prodrug design ideas for central nervous system delivery, *Molecular pharmaceutics* 8(5) (2011) 1857-66.
- [32] X. Gao, L. Zhou, X. Jiao, F. Lu, C. Yan, X. Zeng, J. Wang, Y. Shi, Mechanism of substrate recognition and transport by an amino acid antiporter, *Nature* 463(7282) (2010) 828-32.
- [33] X. Gao, F. Lu, L. Zhou, S. Dang, L. Sun, X. Li, J. Wang, Y. Shi, Structure and mechanism of an amino acid antiporter, *Science* 324(5934) (2009) 1565-8.
- [34] Y. Fang, H. Jayaram, T. Shane, L. Kolmakova-Partensky, F. Wu, C. Williams, Y. Xiong, C. Miller, Structure of a prokaryotic virtual proton pump at 3.2 Å resolution, *Nature* 460(7258) (2009) 1040-3.

- [35] E. Augustyn, K. Finke, A.A. Zur, L. Hansen, N. Heeren, H.C. Chien, L. Lin, K.M. Giacomini, C. Colas, A. Schlessinger, A.A. Thomas, LAT-1 activity of meta-substituted phenylalanine and tyrosine analogs, *Bioorganic & medicinal chemistry letters* 26(11) (2016) 2616-21.
- [36] P. Kongpracha, S. Nagamori, P. Wiriyasermkul, Y. Tanaka, K. Kaneda, S. Okuda, R. Ohgaki, Y. Kanai, Structure-activity relationship of a novel series of inhibitors for cancer type transporter L-type amino acid transporter 1 (LAT1), *Journal of pharmacological sciences* 133(2) (2017) 96-102.
- [37] H. Ylikangas, K. Malmioja, L. Peura, M. Gynther, E.O. Nwachukwu, J. Leppanen, K. Laine, J. Rautio, M. Lahtela-Kakkonen, K.M. Huttunen, A. Poso, Quantitative insight into the design of compounds recognized by the L-type amino acid transporter 1 (LAT1), *ChemMedChem* 9(12) (2014) 2699-707.
- [38] A.A. Zur, H.C. Chien, E. Augustyn, A. Flint, N. Heeren, K. Finke, C. Hernandez, L. Hansen, S. Miller, L. Lin, K.M. Giacomini, C. Colas, A. Schlessinger, A.A. Thomas, LAT1 activity of carboxylic acid bioisosteres: Evaluation of hydroxamic acids as substrates, *Bioorganic & medicinal chemistry letters* 26(20) (2016) 5000-5006.
- [39] T. Albers, W. Marsiglia, T. Thomas, A. Gameiro, C. Grewer, Defining substrate and blocker activity of alanine-serine-cysteine transporter 2 (ASCT2) Ligands with Novel Serine Analogs, *Molecular pharmacology* 81(3) (2012) 356-65.
- [40] L.A. Cynober, Plasma amino acid levels with a note on membrane transport: characteristics, regulation, and metabolic significance, *Nutrition* 18(9) (2002) 761-6.
- [41] L.S. Konstantinova, O.I. Bol'shakov, N.V. Obruchnikova, H. Laborie, A. Tanga, V. Sopena, I. Lanneluc, L. Picot, S. Sable, V. Thiery, O.A. Rakitin, One-pot synthesis of 5-phenylimino, 5-thieno or 5-oxo-1,2,3-dithiazoles and evaluation of their antimicrobial and antitumor activity, *Bioorganic & medicinal chemistry letters* 19(1) (2009) 136-41.
- [42] J.H. Appel R., Haller I., Plempel M., 1,2,3-Dithiazolderivate, Verfahren zu ihrer Herstellung Sowie ihre Verwendung als Arzneimittel, DE Pat. 2848221 (1980).
- [43] R.C.W. Besson T., Cottenceau G., Pons A.M., Antimicrobial evaluation of 3,1-benzoxazin-4-ones, 3,1-benzothiazin-4-ones, 4-alkoxyquinazolin-2-carbonitriles and N-arylimino-1,2,3-dithiazoles, *Bioorg. Med. Chem. Lett.* 6 (1996) 2343-2348.
- [44] B.T. Cottenceau G., Gautier V., Rees C.W., Pons A.M., Antibacterial evaluation of novel N-arylimino-1,2,3-dithiazoles and N-arylcyanothioformamides, *Bioorg. Med. Chem. Lett.* 6 (1996) 529-532.
- [45] K. O., Systematic Qsar procedures with quantum chemical descriptors, *Quant. Struct.-Act. Relat.* 6 (1987) 179-184.
- [46] R.O.A. Konstantinova L.S., Synthesis and properties of 1,2,3-dithiazoles, *Russ. Chem. Rev.* 77 (2008) 521-546.
- [47] F.E. Mayer R., Mataushek B., Verfahren zur Herstellung von Aromatisch oder Heteroaromatisch Substituierten Cyanthioformamiden, DD Pat. 212387 (1984).
- [48] R.C.W. Thiery V., Besson T., Cottenceau G., Pons A.M., Antimicrobial activity of novel N-quinolinyll and N-naphthylimino-1,2,3-dithiazoles, *Eur. J. Med. Chem.* 33 (1998) 149-153.
- [49] J.E. Moore, Certain 4-Halo-5-aryl-1,2,3-dithiazole Compounds and their Preparation, US Pat. 4059590 (1977).

Legends to Figures

Fig. 1. Dose-response curves for the inhibition of the recombinant hLAT1 in proteoliposomes.

Transport was measured adding 5 μM [^3H]His to proteoliposomes containing 10 mM His in the presence of different concentrations of the indicated compounds and measured in 15 min as described in Materials and Methods. Dose-response for compound **5** (A), compound **10** (B), compound **11** (C), compound **12** (D), compound **16** (E), compound **17** (F), compound **19** (G) and

1 compound **59** (H). Percent residual activity with respect to the control (without additions) is
2 reported. Results are mean \pm S.D. from three independent experiments.
3

4 **Fig. 2.** Possible pathways for the mechanism of hLAT1 transporter inhibition by compounds. Cys-
5 S, thiolate group of a Cys residue.
6
7

8 **Fig. 3.** Sketch of experimental design for assessing the possible reaction of the compound with thiol
9 residues of the protein. After reconstitution, proteoliposomes were incubated with DMSO (control)
10 or with a specific compound (Inhibition assay) for the indicated time. Successively these samples
11 were incubated with buffer alone or with 50 mM DTE. Transport was then measured in 30 min by
12 adding 5 μ M [3 H]His to proteoliposomes, as described in Materials and Methods.
13
14
15
16
17
18
19
20

21 ¹: A first size exclusion chromatography was performed to remove the external substrate after
22 reconstitution.
23
24

25 ²: A second size exclusion chromatography was performed to remove inhibitor not bound to the
26 transporter.
27
28
29
30

31 **Fig. 4.** Effect of DTE on the inhibition of [3 H]His uptake in proteoliposomes reconstituted with
32 recombinant hLAT1. Experimental procedure is described in the legend of Fig. 3. Proteoliposomes
33 were incubated with DMSO or with 1.2 μ M compound **5** (A), 1.2 μ M compound **17** (B), and not
34 treated or treated with 50 mM DTE. Results are mean \pm S.D. from three independent experiments.
35
36
37
38
39
40
41 Student's two tailed unpaired t-test was performed on the sample without added compounds
42 (control); p value was symbolized as follows: *p < 0.01.
43
44
45

46 **Fig. 5.** Kinetic analysis of the inhibition of recombinant hLAT1 reconstituted in proteoliposomes.
47 Data were plotted according to Lineweaver–Burk as reciprocal transport rate vs reciprocal His
48 concentration. Transport rate was measured by adding [3 H]His at the indicated concentrations to
49 proteoliposomes containing 10 mM His and stopping the reaction after 15 min as described in
50 Materials and Methods. In (A) 0.8 μ M (\bullet) or 1.2 μ M (\square) **5** was added as inhibitor in comparison to
51 samples without inhibitor (\circ). In (B) 0.8 μ M (\bullet) or 1.2 μ M (\square) **17** was added as inhibitor in
52 comparison to samples without inhibitor (\circ). Results are mean \pm S.D. from three independent
53
54
55
56
57
58
59
60
61
62
63
64
65

1 experiments. (C) Protection of inhibition by substrate. Proteoliposomes reconstituted as described in
2 Materials and Methods, were incubated or not with compound **5** in the presence or absence of **5** or
3
4 10 mM His. After incubation, samples were subjected to size exclusion chromatography to remove
5
6 the unreacted inhibitor and substrate; transport rate was measured adding 5 μM [^3H]His. The
7
8 reaction was stopped after 30 min as described in Materials and Methods. Percent residual activity
9
10 with respect to the control (without additions) is reported. Results are mean \pm S.D. from three
11
12 independent experiments. Student's two tailed unpaired t-test was performed on the sample without
13
14 added compounds (control); p value was symbolized in (C) as follows: *p < 0.01.
15
16
17
18

19 **Fig. 6.** Best docking poses of the two selected compounds obtained through covalent docking on
20
21 LAT1 homology model. LAT1 in its outward-open conformation is shown as ribbon; the gate
22
23 residue Phe252 is shown in stick representation. Compounds **5** and **17** covalently docked to residue
24
25 Cys407 are shown in stick representation in A and B, respectively.
26
27
28

29 **Fig. 7.** Inhibition analysis of compound **5** on recombinant hLAT1 mutants reconstituted in
30
31 proteoliposomes. Dose-response curve for the inhibition of compound **5** on LAT1 C407A (A), on
32
33 C335A (B) and on double mutant C335A/C407A (C). Transport was measured by adding 5 μM
34
35 [^3H]His to proteoliposomes containing 10 mM His in the presence of different concentrations of the
36
37 compound added together with [^3H]His and measured in 30 min as described in Materials and
38
39 Methods. Percent residual activity with respect to the control (without additions) is reported.
40
41 Results are mean \pm S.D. from three independent experiments.
42
43
44
45

46 **Fig. 8.** Effect of compound **5** on transport activity in intact cells. (A) Western Blot analysis was
47
48 conducted using anti-HA antibody on cells transfected with empty vector (pCDNA3) or hLAT1-HA
49
50 (pCDNA3-LAT1) as described in Materials and Methods. Actin is used as loading control. Picture
51
52 is representative of three independent experiments. (B) HEK293 cells were cultured and transfected
53
54 with pCDNA3-hLAT1-HA as described in Materials and Methods and used for transport adding 5
55
56 μM [^3H]His and 1 μM of compound **5**. Transport was stopped after 1 min as described in Materials
57
58 and Methods. Results are mean \pm S.D. from three independent experiments. Student's two tailed
59
60
61
62
63
64
65

unpaired t-test was performed on the sample without added compound (control); p value was symbolized as follows: *p < 0.01.

Fig. 9. Effect of compounds on cell viability. SiHa cells were cultured in 6 well plates as described in Materials and Methods. Compounds **5** (A), **17** (B) and **51** (C) were added at the indicated concentrations and pictures were taken after 24 h and 48 h of treatment. As negative control, DMSO was added. After 48h medium was replaced with fresh DMEM without inhibitors (wash) and pictures were taken after 24h. Picture is representative of three independent experiments.

Figure 1
[Click here to download high resolution image](#)

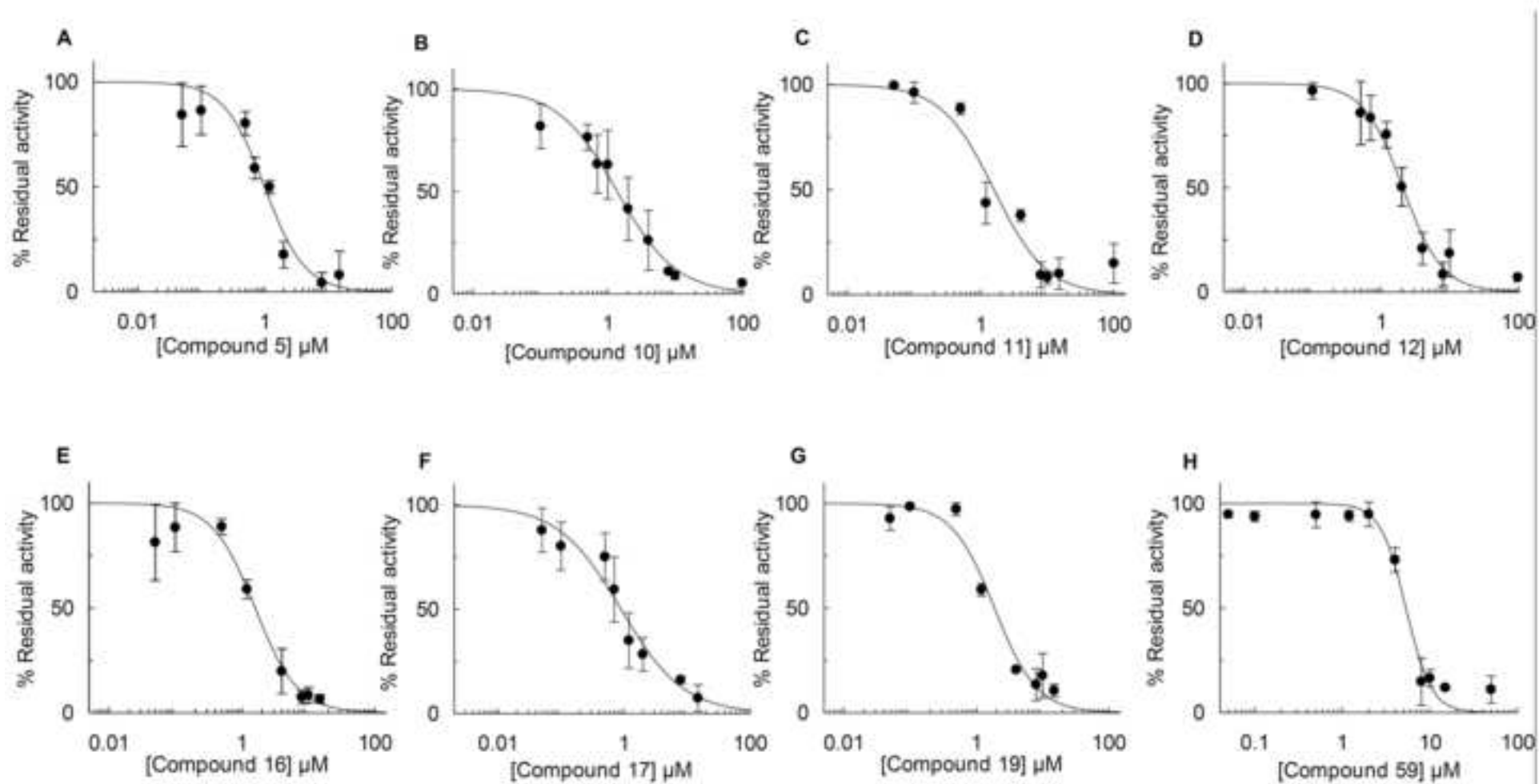


Figure 2
[Click here to download high resolution image](#)

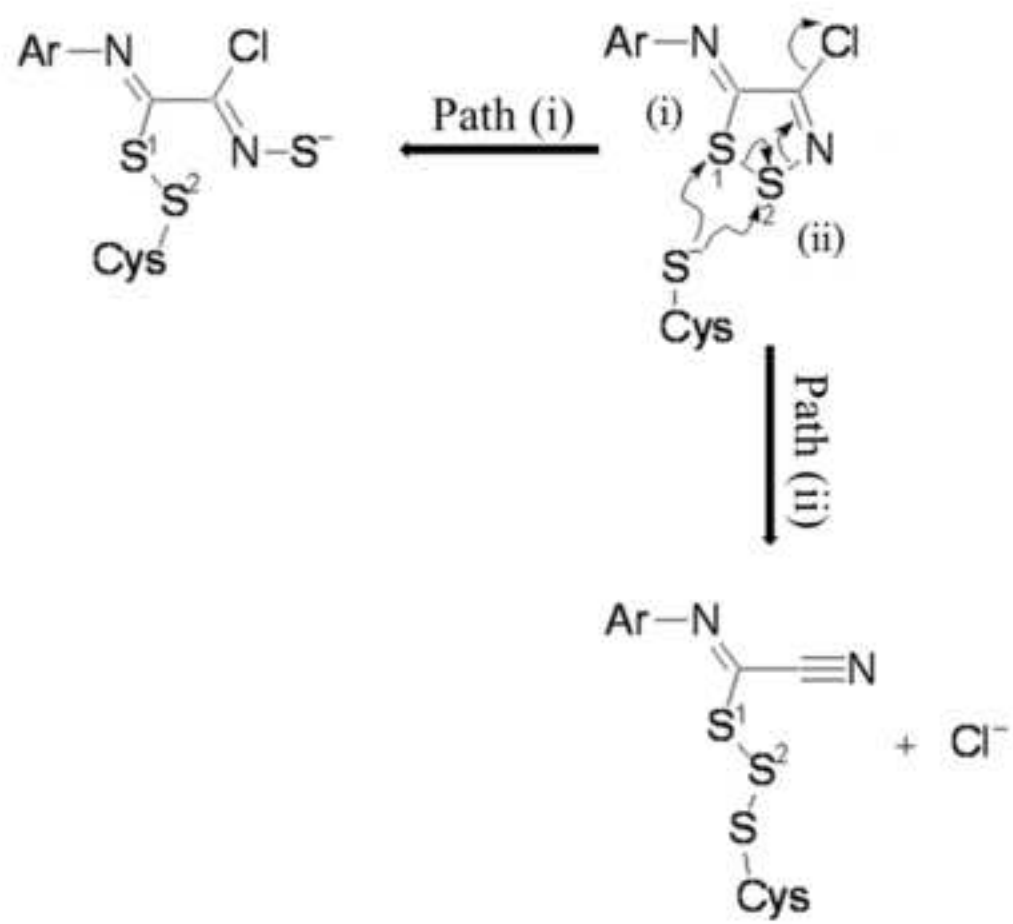
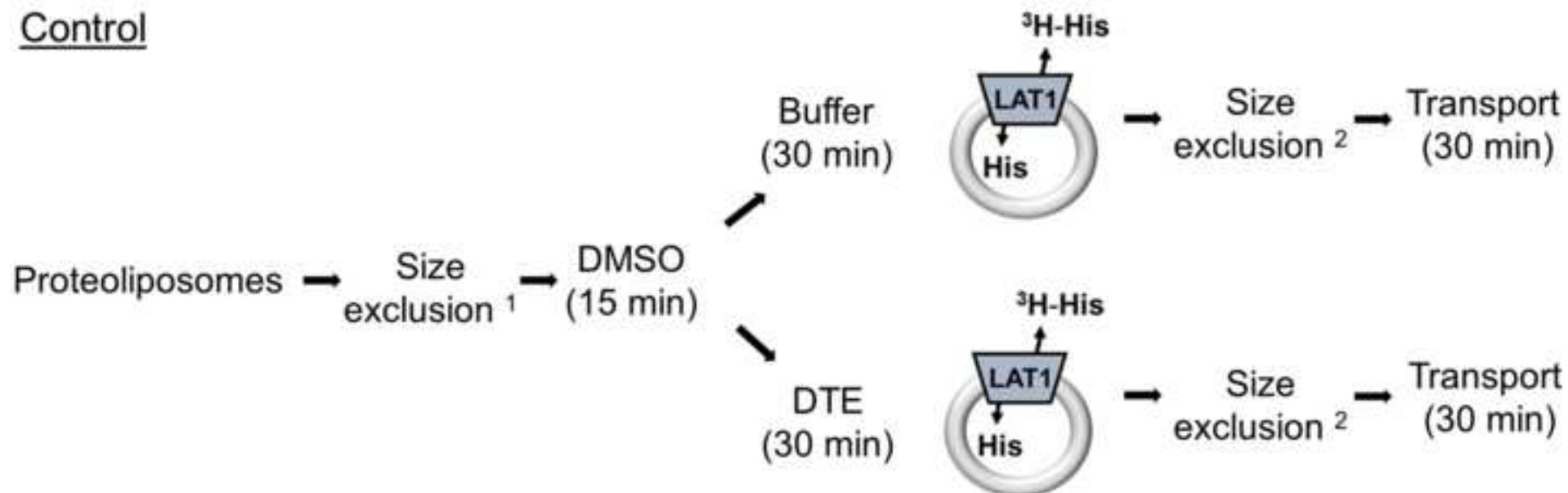


Figure 3
[Click here to download high resolution image](#)

Control



Inhibitor assay

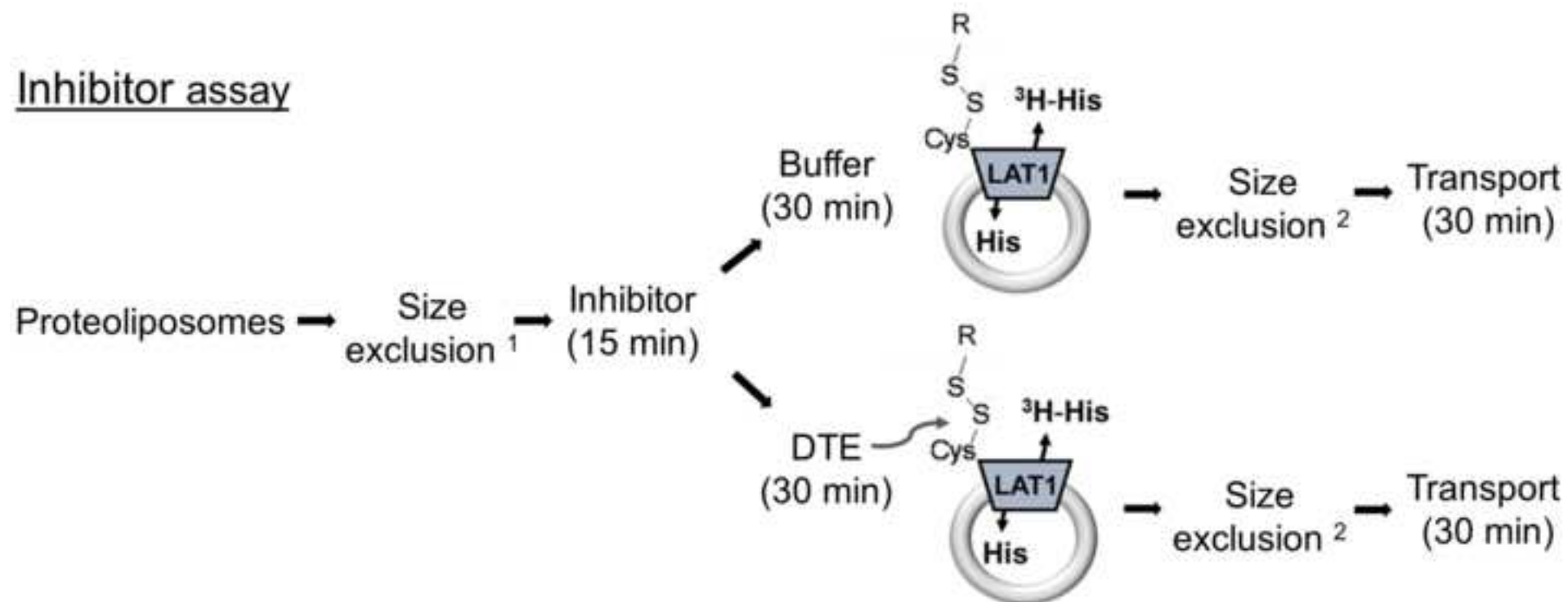


Figure 4A
[Click here to download high resolution image](#)

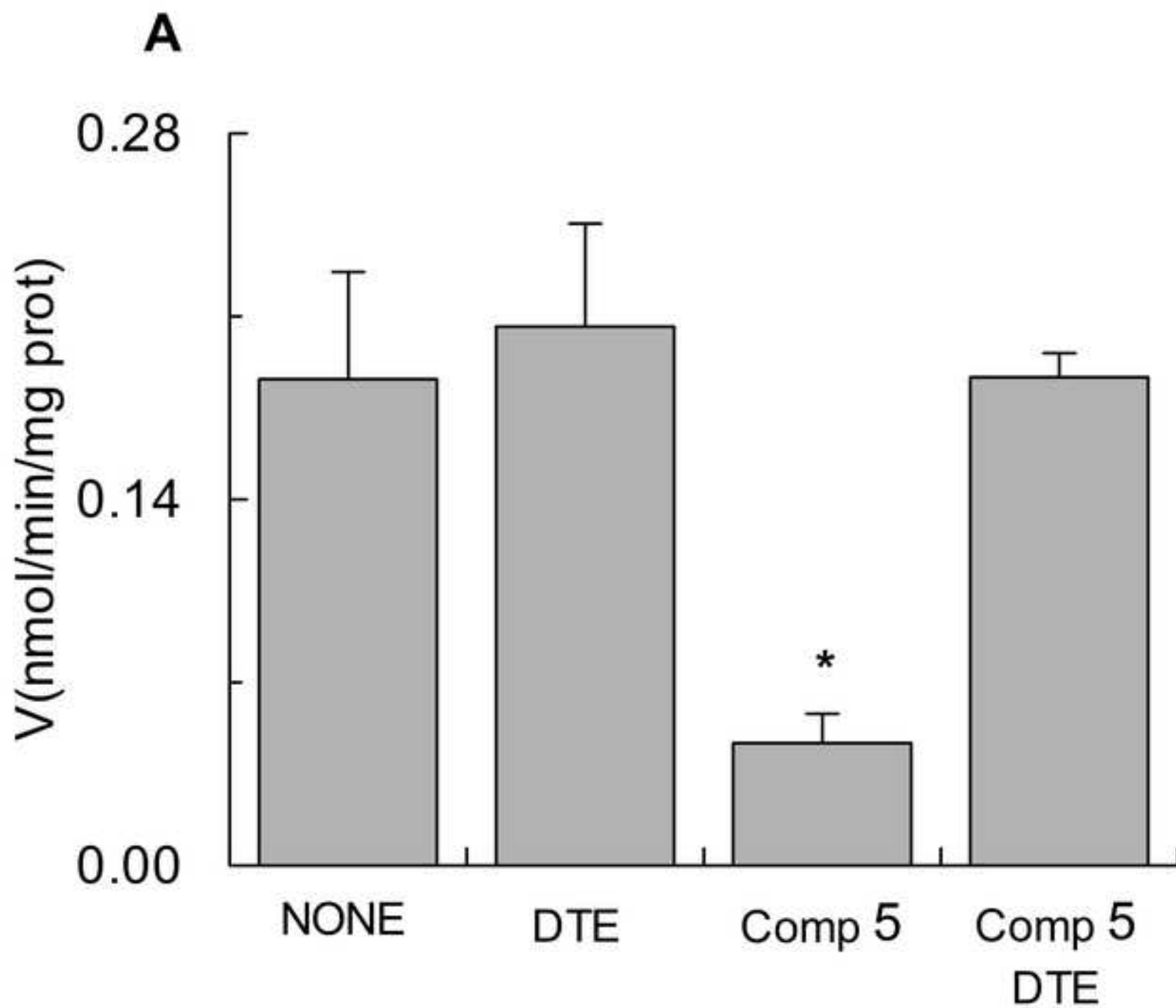


Figure 4B
[Click here to download high resolution image](#)

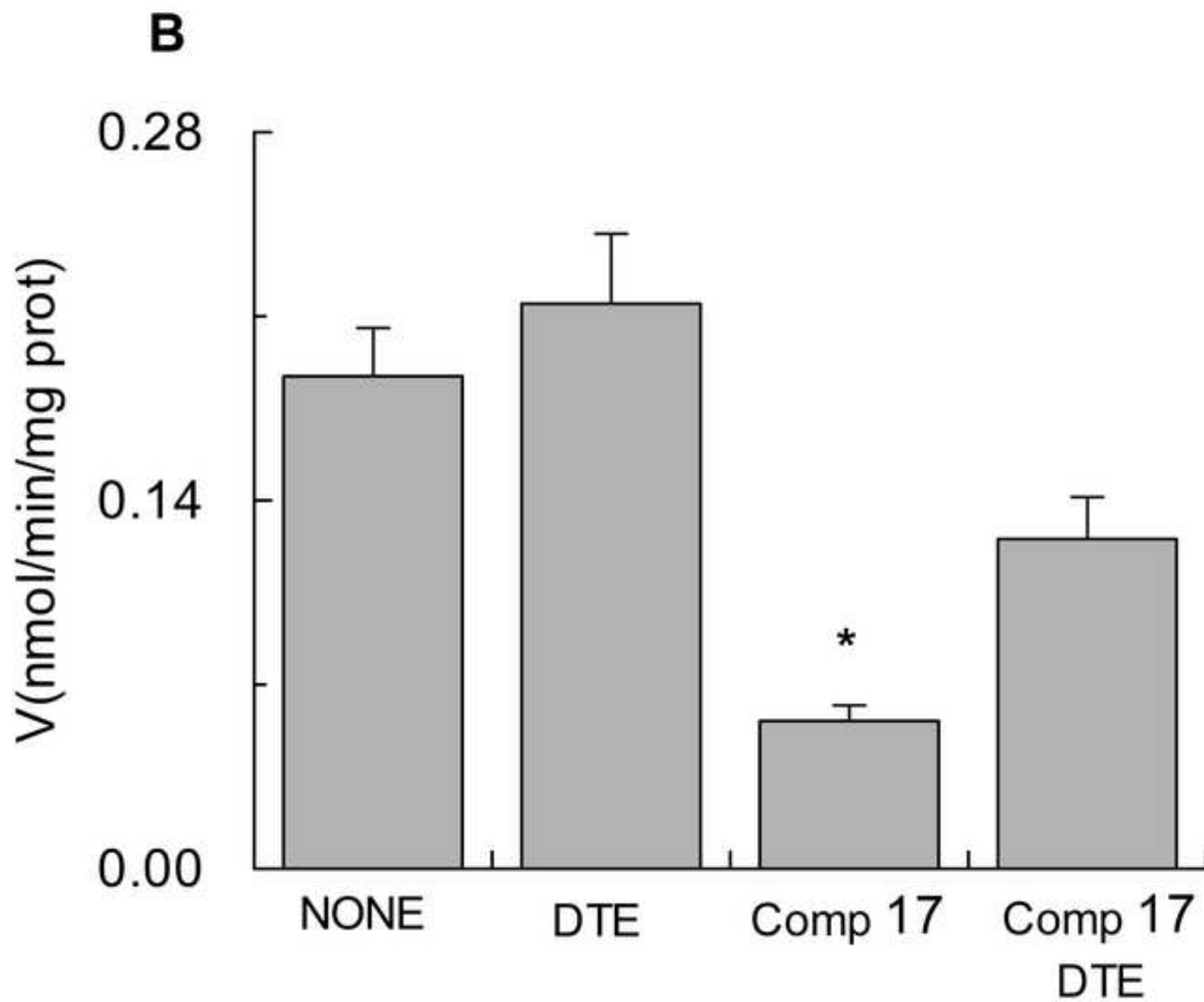


Figure 5A
[Click here to download high resolution image](#)

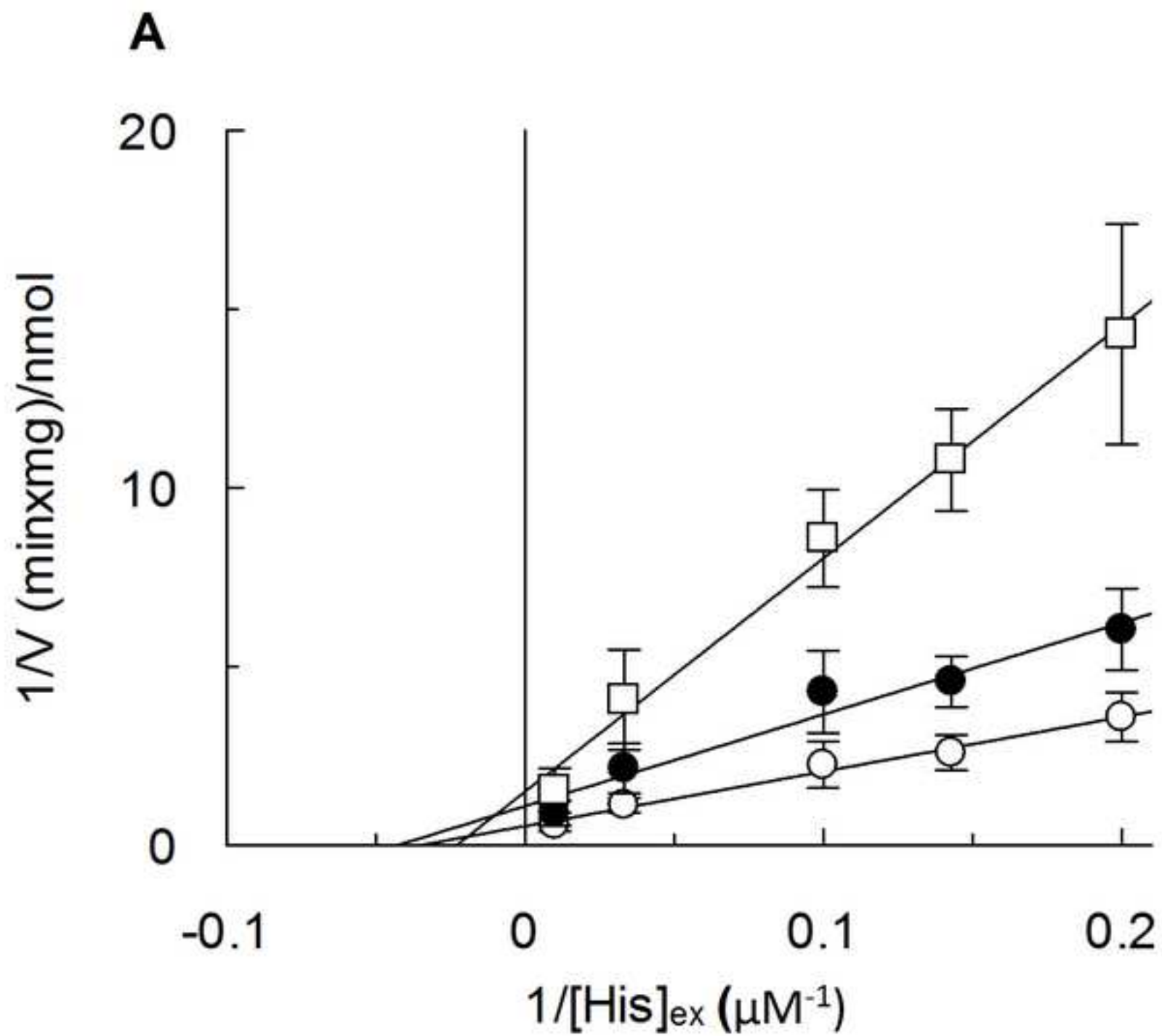


Figure 5B
[Click here to download high resolution image](#)

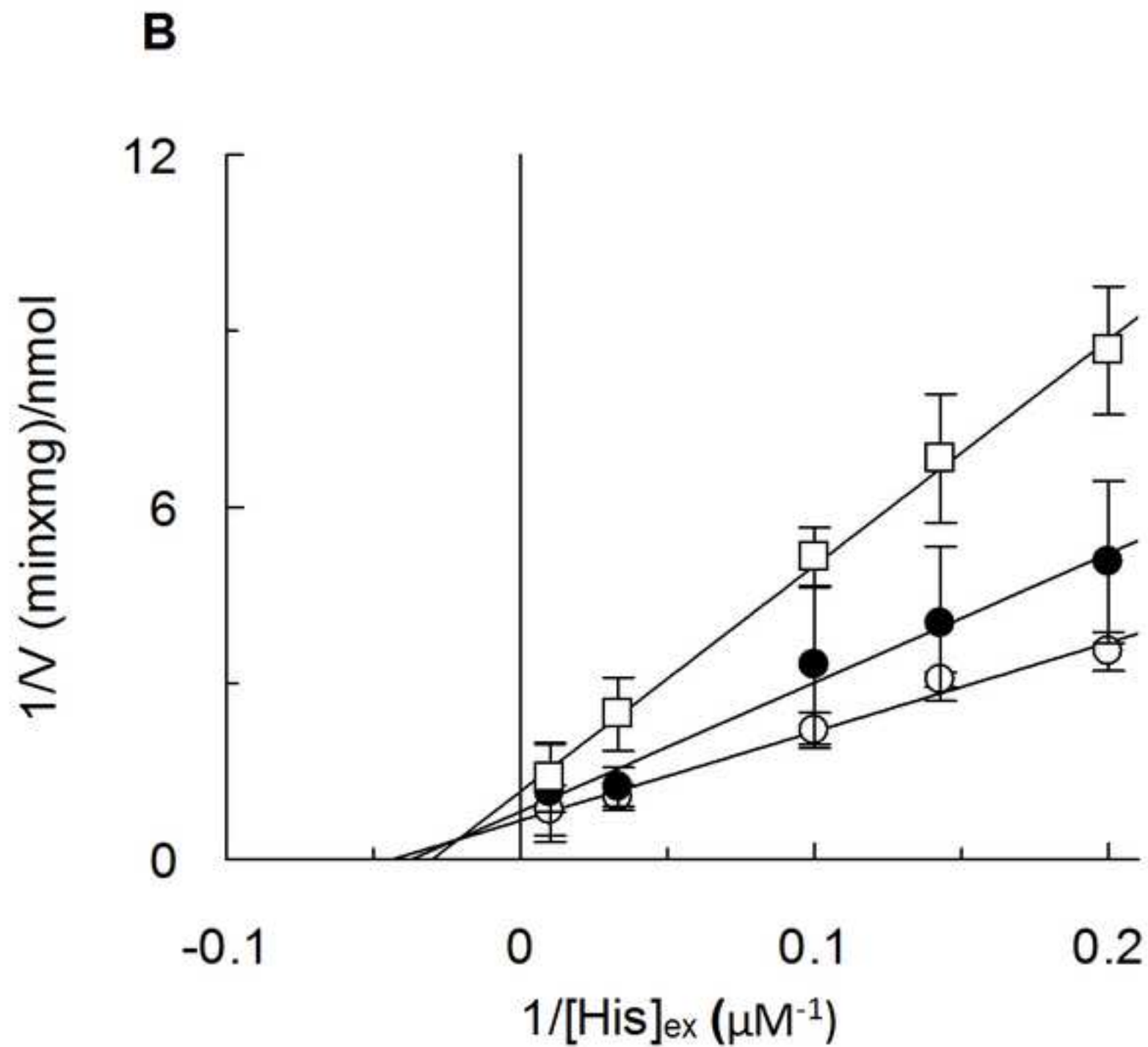


Figure 5C
[Click here to download high resolution image](#)

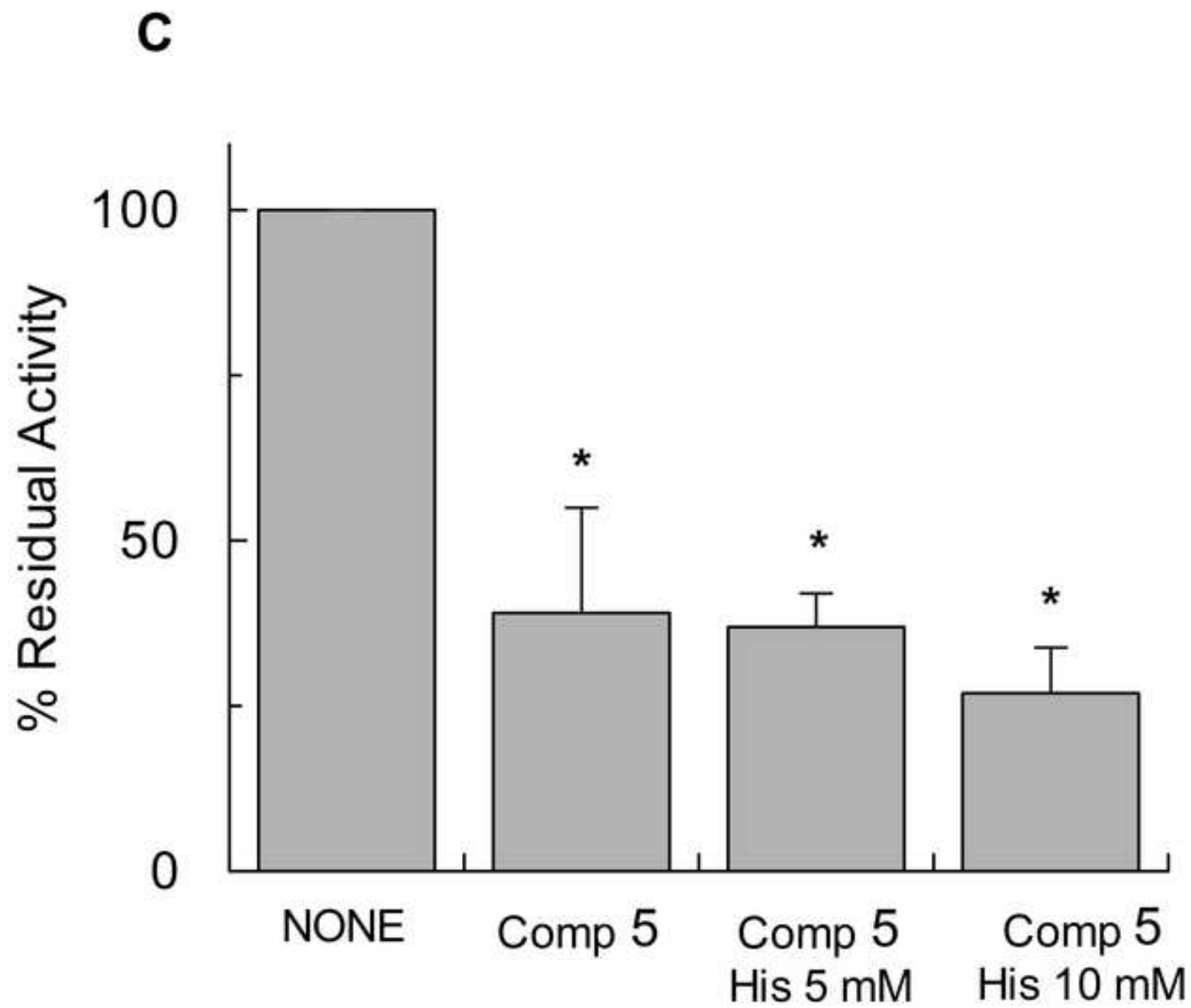


Figure 6
[Click here to download high resolution image](#)

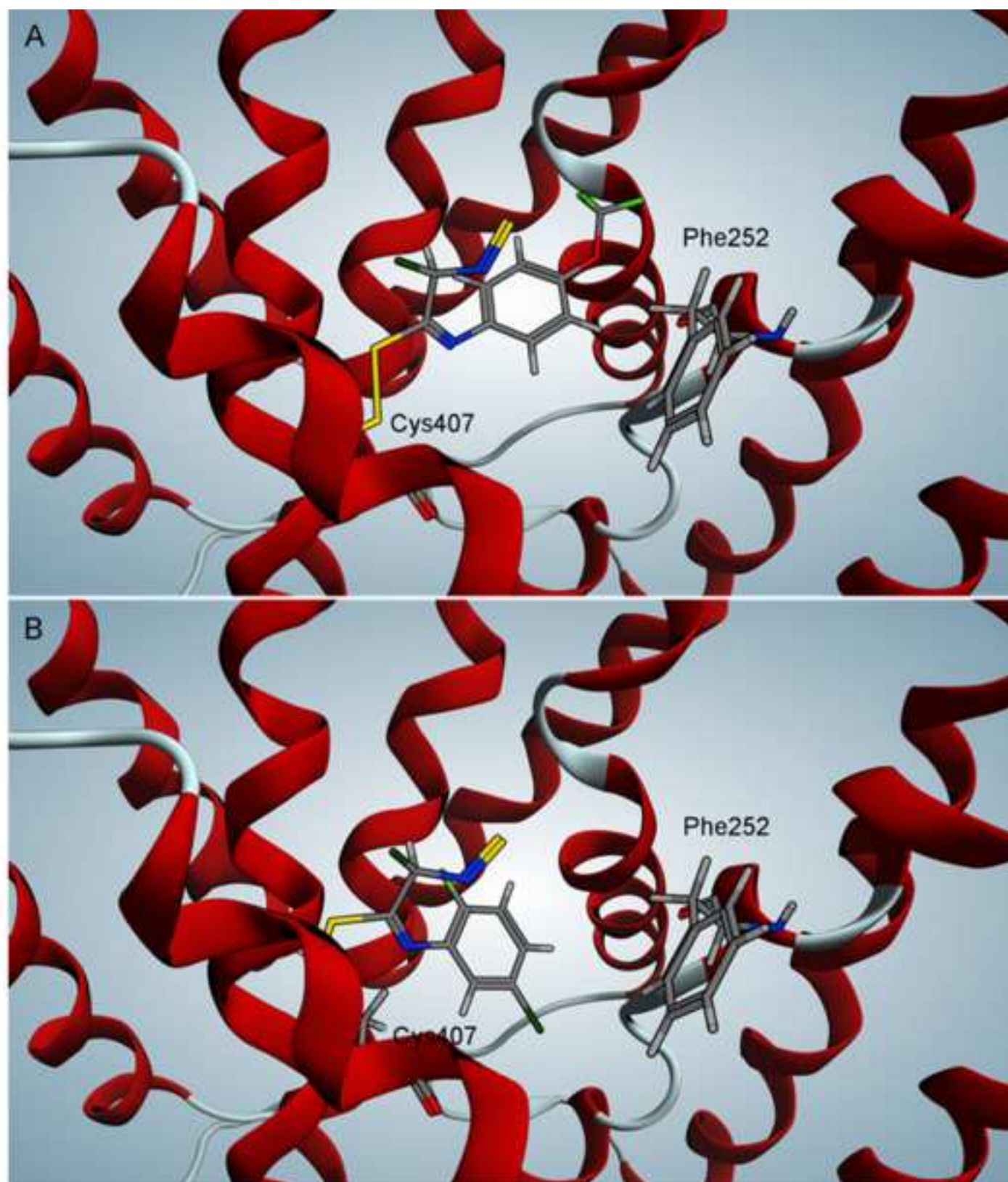


Figure 7A
[Click here to download high resolution image](#)

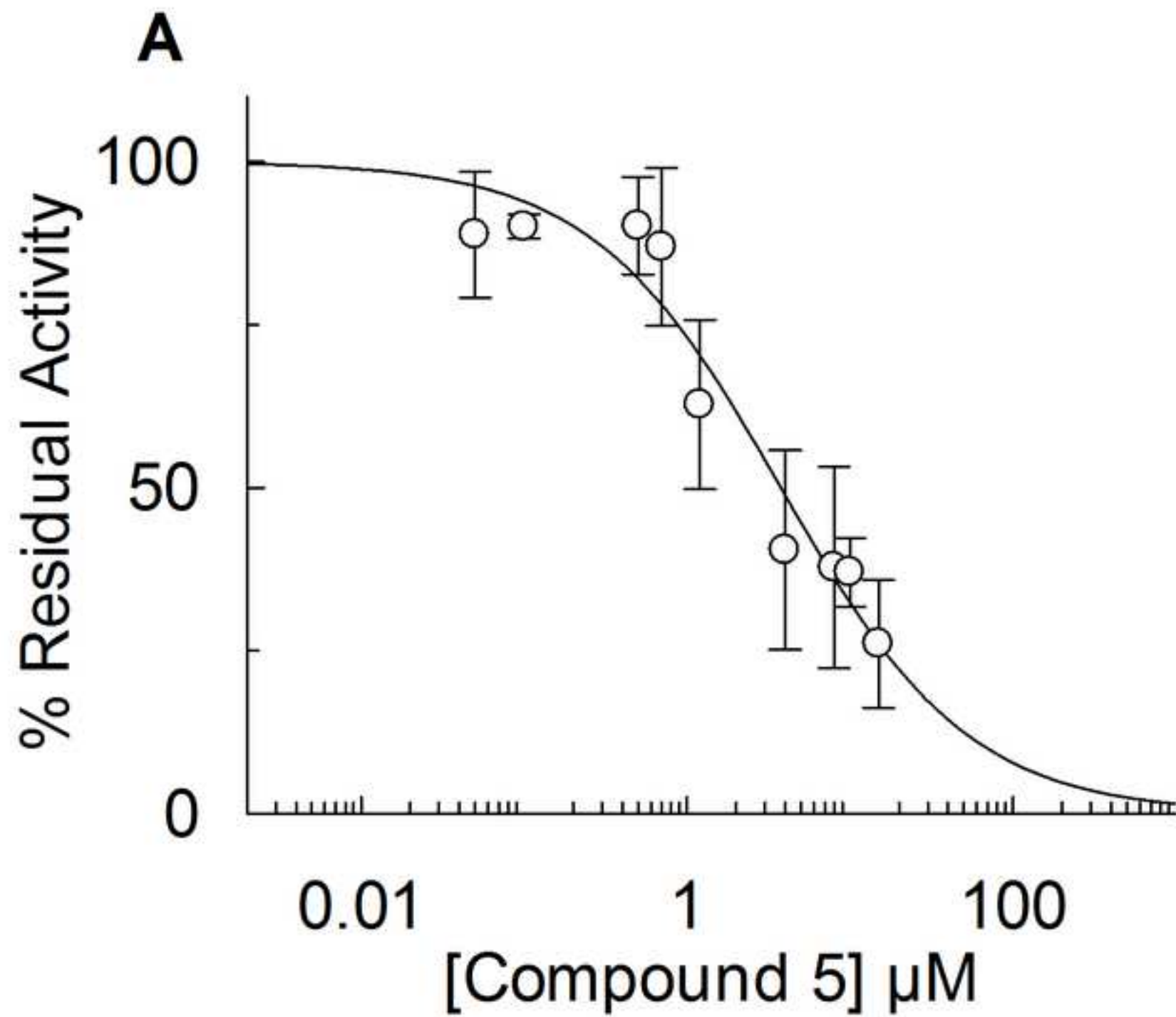


Figure 7B
[Click here to download high resolution image](#)

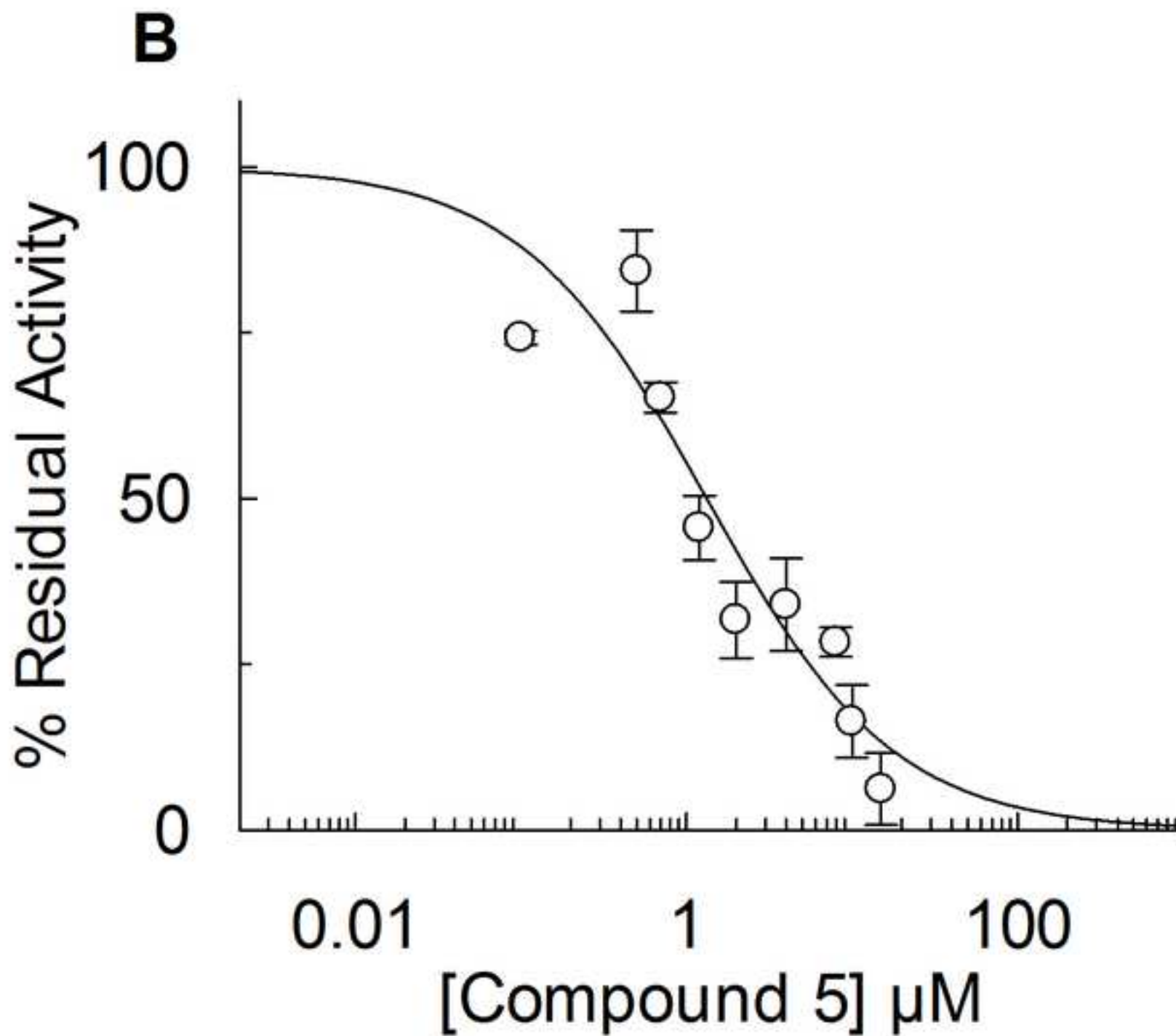


Figure 7C
[Click here to download high resolution image](#)

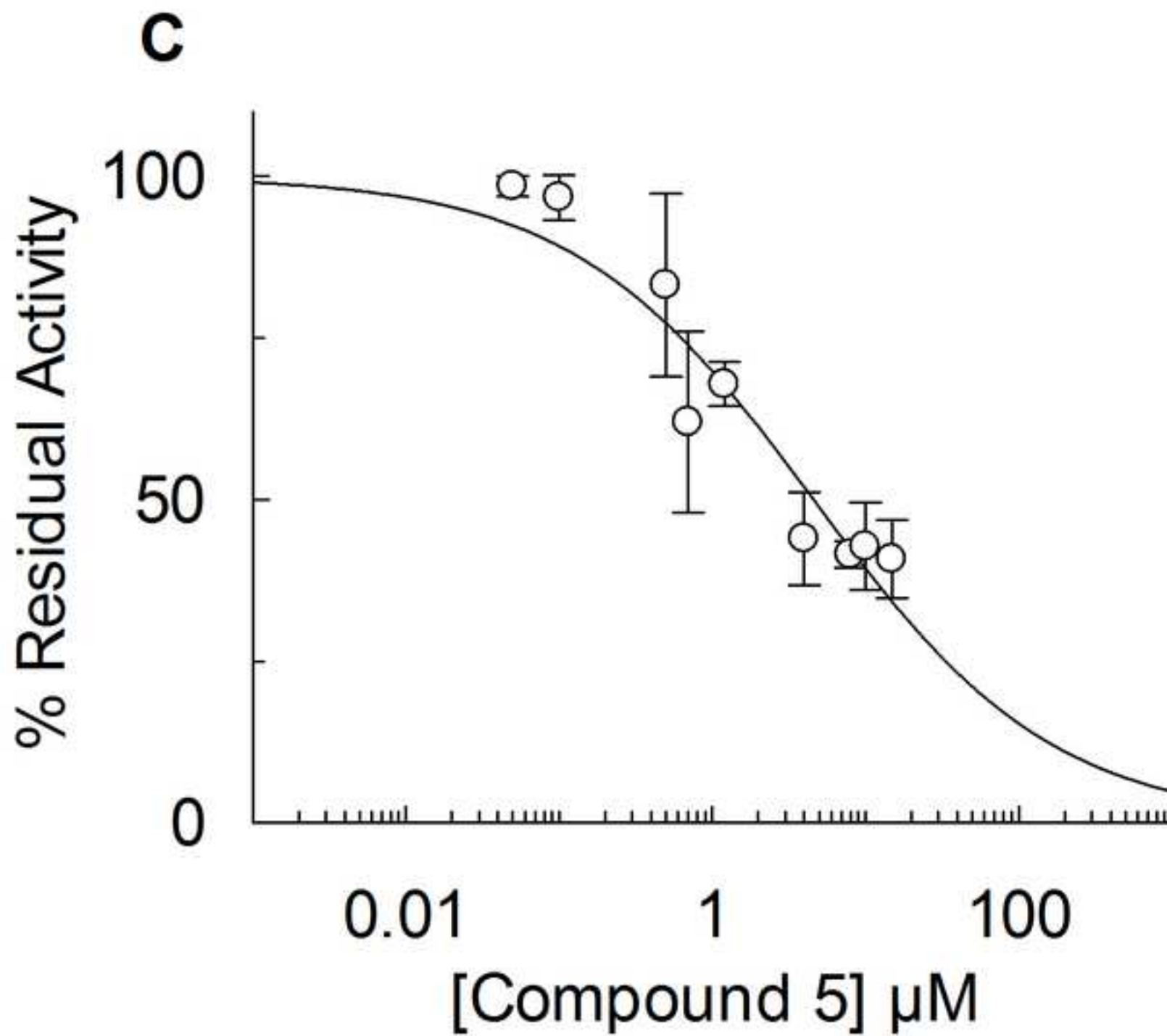
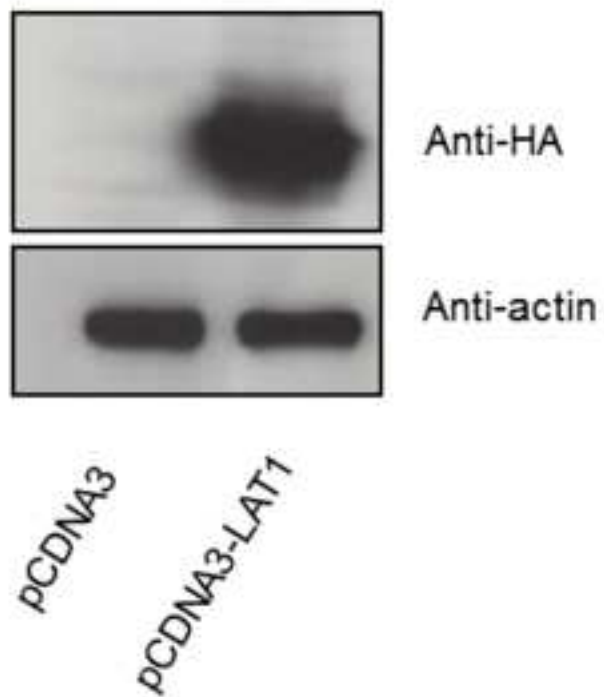


Figure 8
[Click here to download high resolution image](#)

A



B

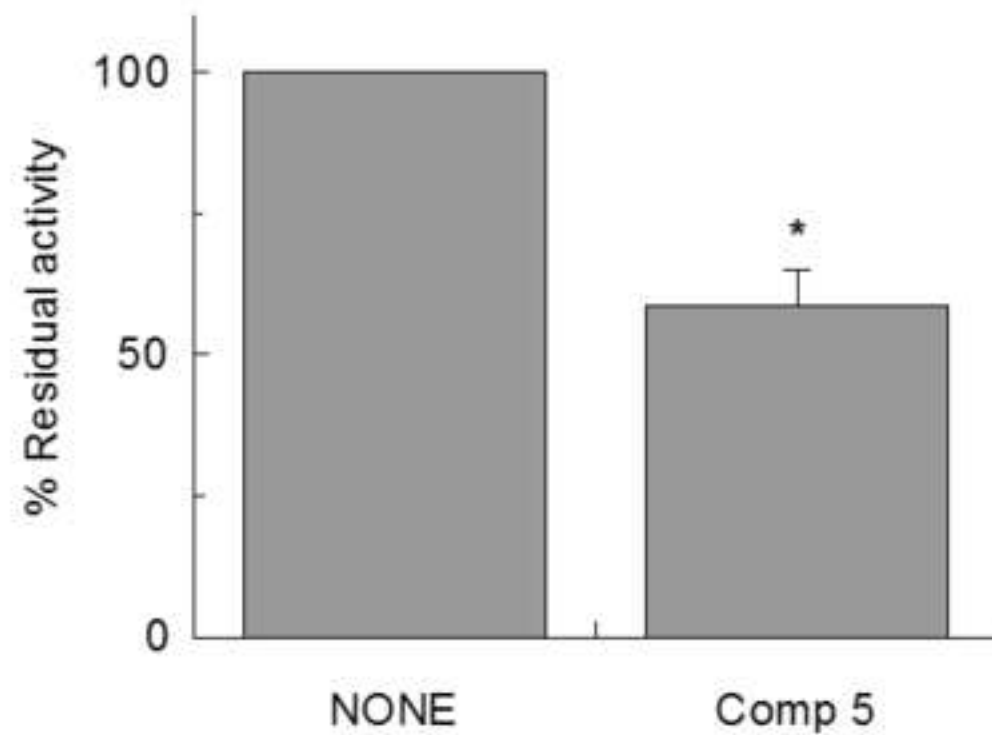


Figure 9A
[Click here to download high resolution image](#)

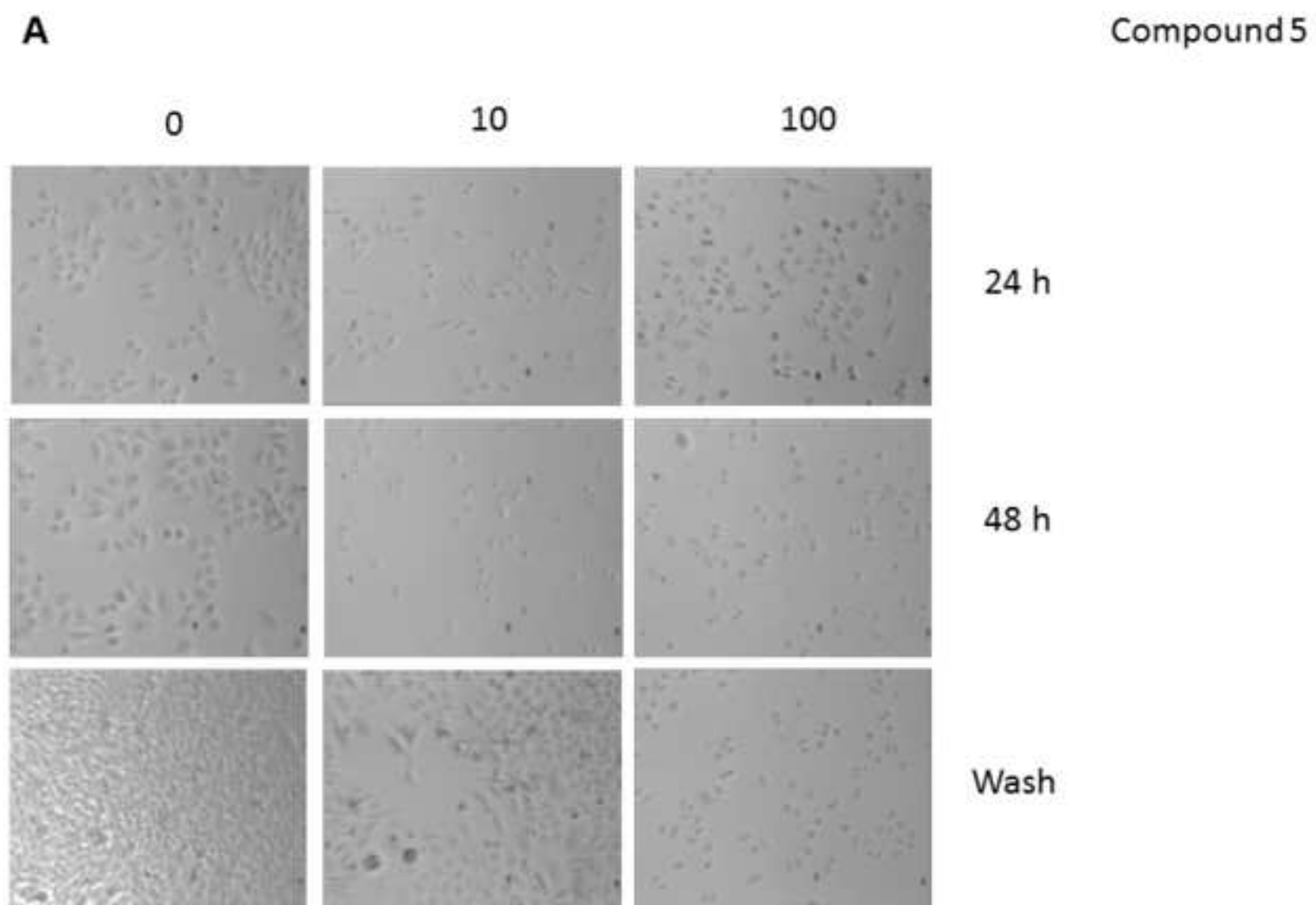


Figure 9B
[Click here to download high resolution image](#)

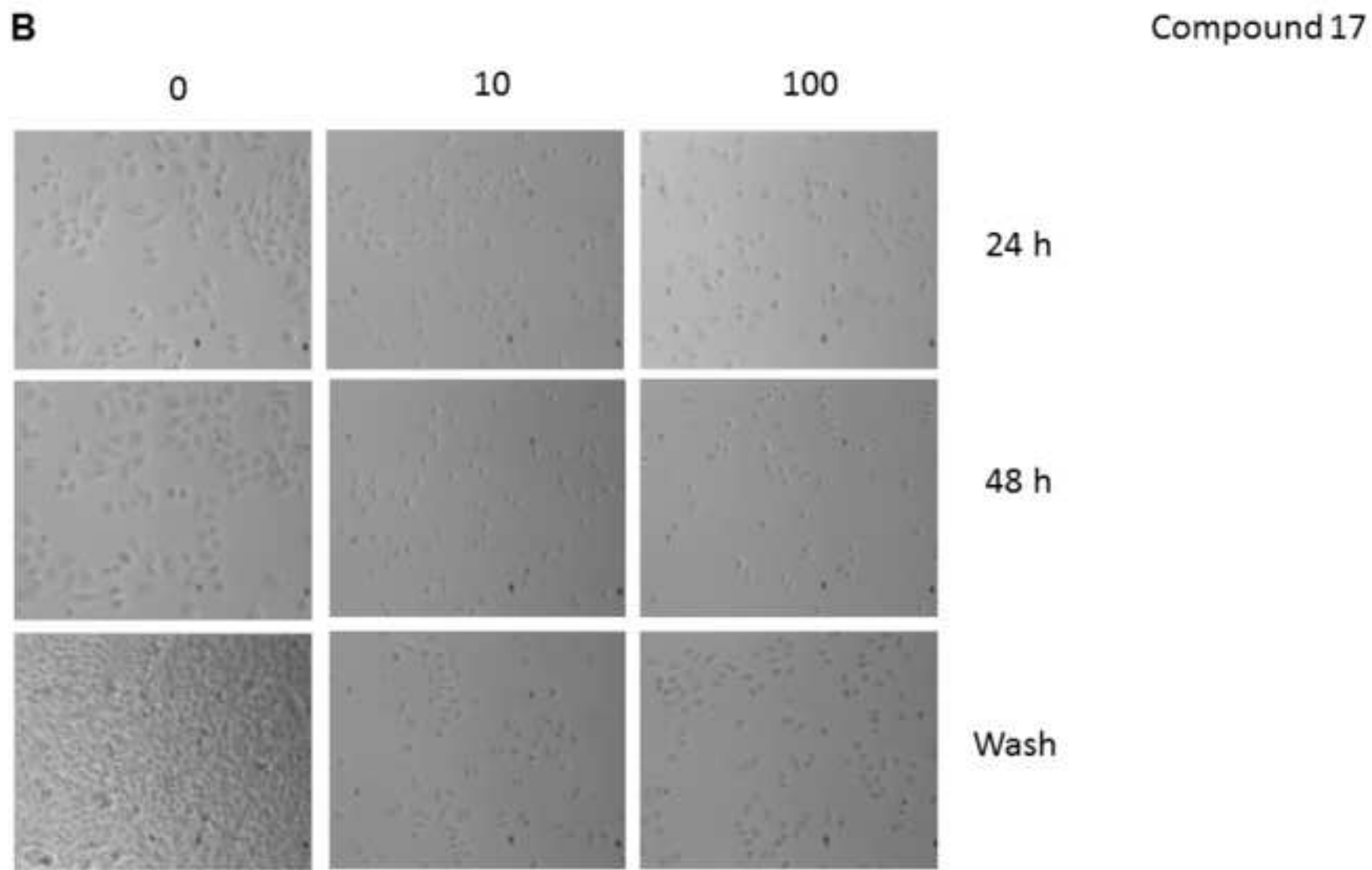
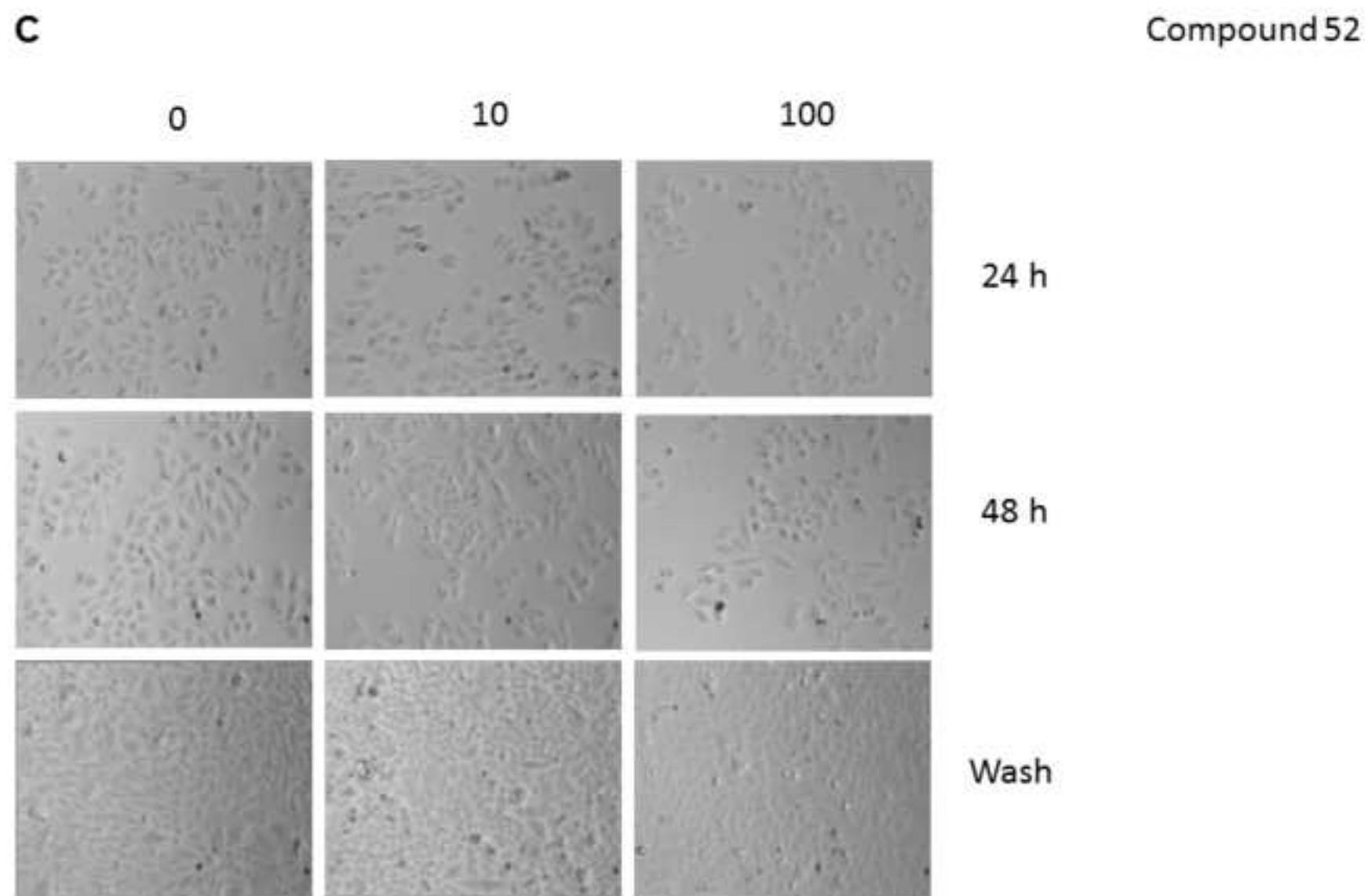
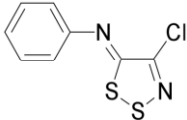
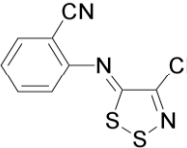
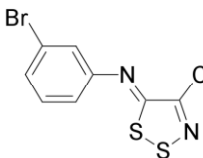
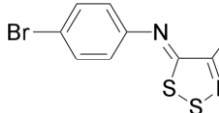
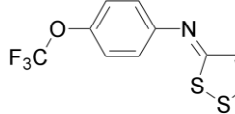
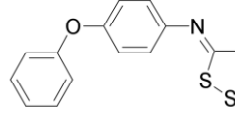
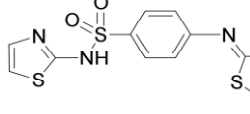
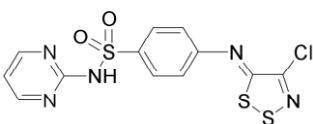
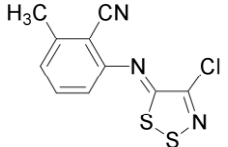
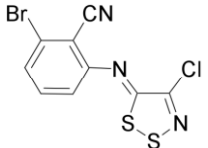
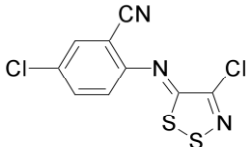
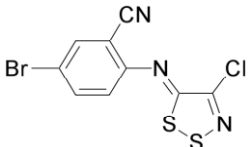
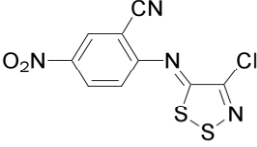
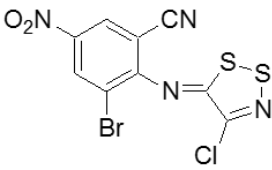
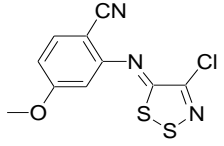
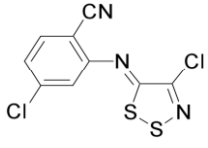
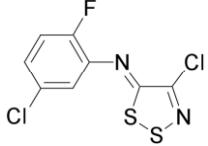


Figure 9C
[Click here to download high resolution image](#)

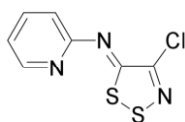


Entry	Structure	%Inhibition at 100 μM
1		81-82
2		44-45
3		82-83
4		68-69
5		> 90
6		62-63
7		63-64

8		81-82
9		63-64
10		> 90
11		> 90
12		> 90
13		88-89
14		85-86
15		85-86
16		> 90
17		> 90

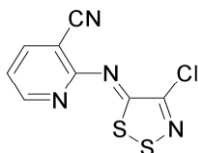
18		78-79
19		> 90
20		68-71
21		31-33
22		67-69
23		49-51
24		83-84
25		65-66

26



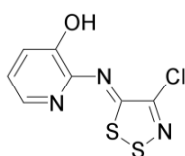
4-9

27



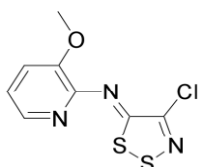
41-49

28



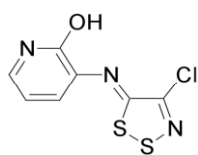
35-45

29



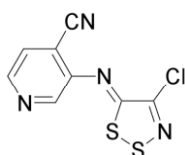
10-15

30



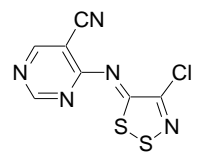
67-68

31



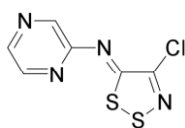
87-89

32

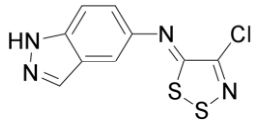
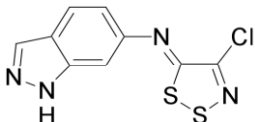
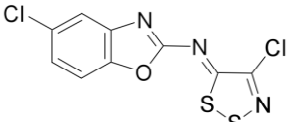
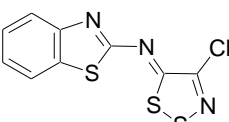
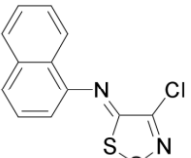
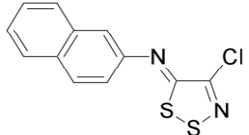
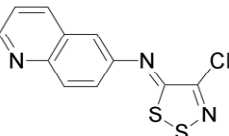
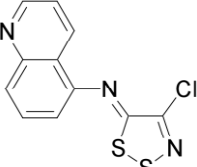
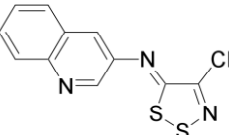
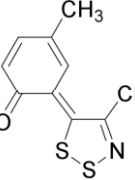


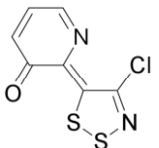
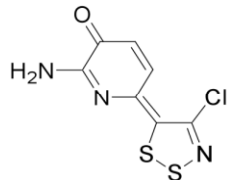
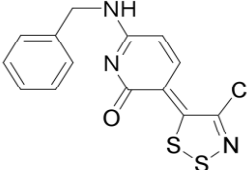
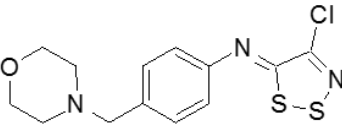
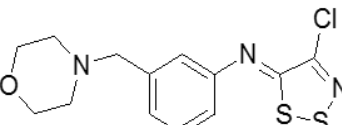
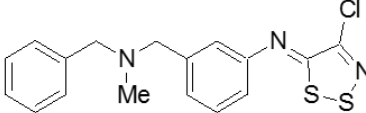
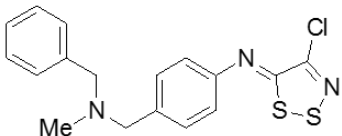
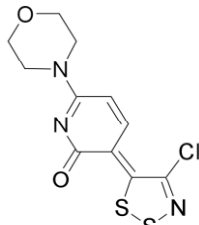
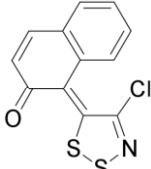
75-79

33



63-66

34		29-31
35		48-49
36		66-67
37		67-68
38		59-61
39		58-59
40		74-75
41		65-66
42		84-85
43		70-71

44		48-49
45		63-66
46		66-69
47		61-62
48		58-59
49		51-52
50		48-49
51		26-30
52		72-73

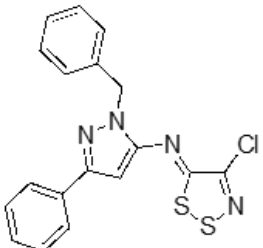
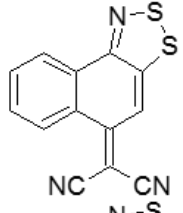
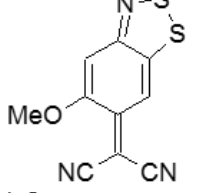
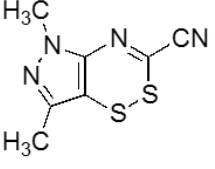
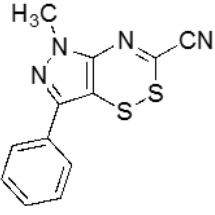

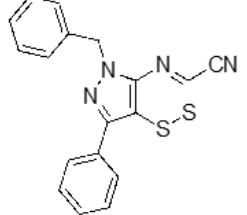
53		48-49
54		60-62
55		0
56		88-89
57		71-72
58		77-78
59		> 90

Table 1

Inhibition of hLAT1 by 1,2,3-dithiazoles **1-55** and 1,2,4-dithiazines **56-59**.

Compounds structures (1-59) prepared as described in Materials and Methods were tested as inhibitors of hLAT1 at 100 μ M concentration. Transport activity was assayed in proteoliposomes as [3 H]His_{ex}/His_{in} antiport as described in Materials and Methods. Percentage of inhibition from two experiments are reported (see section 2.10). > 90% is reported in case of both values higher than 90%.

